Wave Energy for Seawater Desalination

Hydraulic Coupling of Heaving and Surge Wave Energy Converters to Reverse Osmosis: A Numerical Study Across Sea States

OE54035: ODE MSc Thesis

Pranjal Bhushan

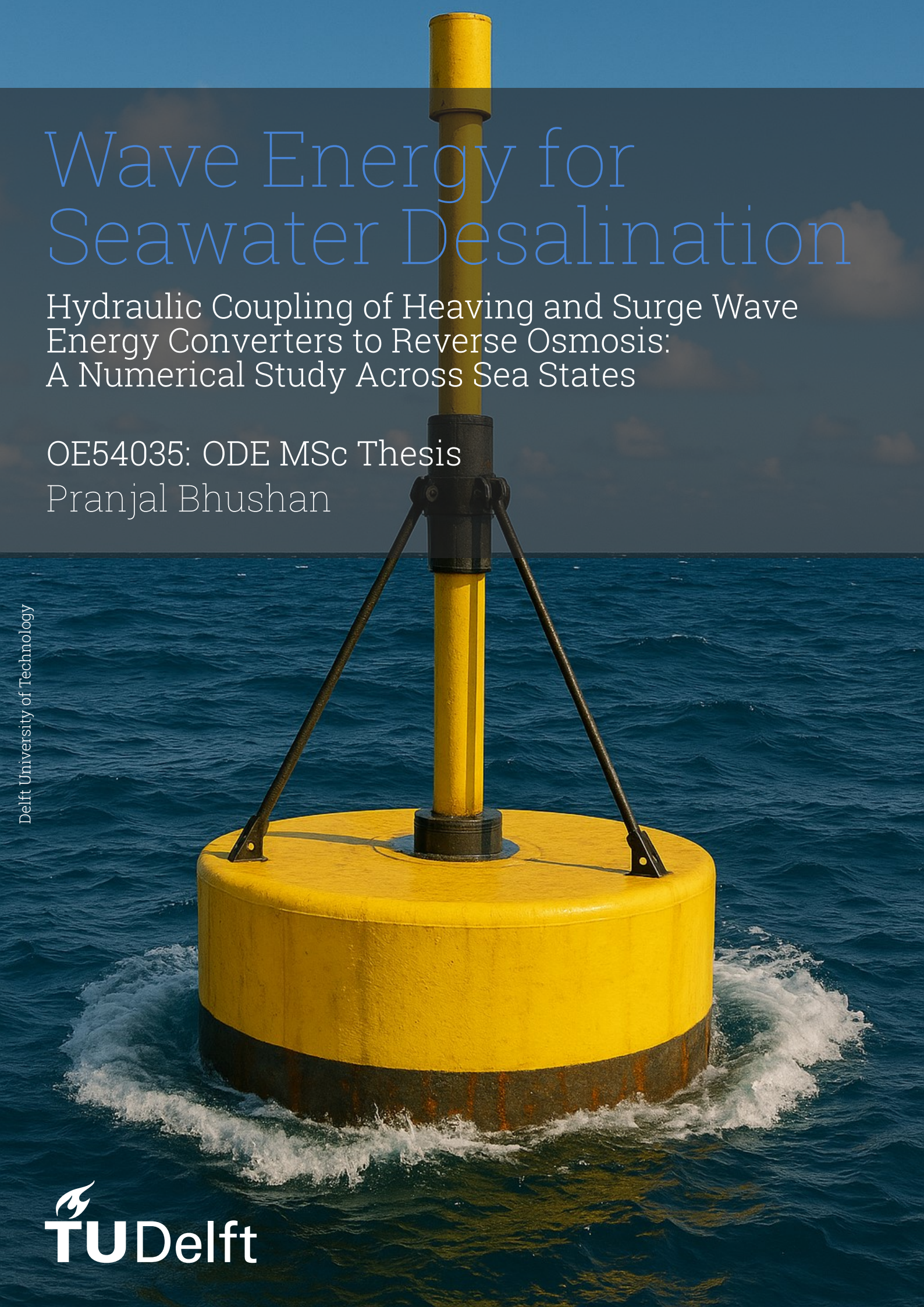

Delft University of Technology

TU Delft

Wave Energy for Seawater Desalination

Hydraulic Coupling of Heaving and Surge Wave Energy Converters to Reverse Osmosis: A Numerical Study Across Sea States

by

Pranjal Bhushan

to obtain the degree of Master of Science

at the Delft University of Technology,

to be defended publicly on Thursday July 31, 2025 at 02:00 PM.

Student number:	6062091	
Project duration:	November 18, 2024 – June 27, 2025	
Thesis committee:	Dr. Ir. Antonio Jarquin Laguna,	TU Delft, Supervisor
	Dr. Ir. Daniele Fiscaletti,	TU Delft
	Dr. Ir. Jian Tan,	TU Delft

This thesis is confidential and cannot be made public until July 31, 2025.

TU Delft

Acknowledgements

I want to sincerely thank my parents and family for their constant understanding, support, and encouragement during my academic career. Their confidence in me has always given me courage and inspiration, specially during challenging times. I genuinely appreciate all of my friends here, whose support and company have kept me motivated and focused over my academic career. This journey has been much more enjoyable because of their unwavering support.

I want to express my sincere gratitude to my supervisor, Dr. Antonio Laguna, whose advice, insightful feedback, and constant support have been important in determining the goal and quality of this thesis. I really appreciate the time and knowledge that were provided to me during the course of my research. I am also very thankful to my entire thesis committee and all of the instructors of the Section of Offshore and Dredging Engineering at TU Delft for providing me with all the resources I required for my study as well as an engaging academic atmosphere.

The assistance of AI language models for drawing schematic diagrams, clarifying concepts, and drafting outlines is gratefully appreciated.

Lastly, I want to express my gratitude to everyone else who helped with my effort, whether directly or indirectly. The successful completion of my thesis has been greatly aided by your encouragement, guidance, and help.

Pranjal Bhushan
Delft, July 2025

Abstract

This thesis presents two wave energy converters (WECs), an oscillating surge wave energy converter and a heaving point absorber wave energy converter and a reverse osmosis desalination system which are numerically modeled and compared. The primary objective was to assess and contrast their performance in terms of Freshwater Production and Specific Energy Consumption (SEC) over a variety of realistic sea states, which were specified by wave heights (1–5 meters) and wave energy periods (5–9 seconds) incorporating a particular wave spectrum for irregular waves.

An open source MATLAB based solver was used to integrate hydrodynamic data from frequency-domain Boundary Element Method(BEM) solver into time-domain simulations. Both devices harnessed mechanical energy, which was then sent to the reverse osmosis unit via a hydraulic piston configuration. Power matrices displaying SEC, water production and permeate concentration were used to present the results, presenting a direct comparison.

Results showed that the two devices differed significantly. Only in high-energy wave circumstances did the heaving device operate effectively, exhibiting low SEC of 2-4 kWh/m^3 and significant freshwater output in certain sea states. However, in moderate or lower-energy seas, its efficiency significantly decreased. With SEC normally ranging from 2 to 4.5 kWh/m^3 and consistently higher freshwater output, even in milder sea conditions, the oscillating surge device, on the other hand, showed more stable performance. According to the study, the oscillating surge device can provide desalinated water with salt concentrations below the threshold of 600 ppm suggested by the World Health Organization in the majority of sea states, whereas the heaving device often crosses this limit, with the exception of energetic wave conditions. These findings are in good alignment with previous studies on wave-powered desalination.

Limitations include the exclusion of operational issues such as membrane fouling or long-term system degradation, the assumption of linear interpolation for calculating intermediate sea states, and possible errors resulting from simplified models.

The use of complex interpolation techniques to improve accuracy, more simulations over multiple sea states, and experimental validation of results are some suggestions for future research. Additionally, combining environmental and economic evaluations will help in determining if larger-scale deployment of these wave-powered desalination systems is feasible. This study highlights oscillating surge devices as a strong option for sustainable freshwater generation and offers insightful information for enhancing wave energy desalination.

Contents

Nomenclature

Abbreviations

Abbreviation	Definition
BEMIO	Boundary Element Method Input Output
DOF	Degree of Freedom
MCR	Multiple Conditions Run
OSWEC	Oscillating Surge Wave Energy Converter
RM3	Reference Model 3
RO	Reverse Osmosis
SEC	Specific Energy Consumption
WAB	Wave Activated Body
WEC	Wave Energy Converter
WEC-RO	Wave Energy Converter coupled with Reverese Osmosis unit

Symbols

Symbol	Definition	Unit
a	Acceleration	[m/s^2]
g	Acceleration due to Gravity	[m/s^2]
Q	Flow Rate	[m^3/s]
p	Position	[m]
P	Pressure	[Pascal]
v	Velocity	[m/s]
ρ	Density	[kg/m^3]
ω	Frequency	[rad/s]
θ	Incident Wave Angle	[Degree]
τ	Integration Variable	[s]
γ	Peak Enhancement Factor	[-]

1

Introduction

1.1. Background

Freshwater scarcity is a threat to more than two billion people globally, and it is made worse by pollution, climate change, and population growth (UN Water, 2023[38]). The World Health Organization states that drinking water is generally acceptable up to a maximum of 1000 parts per million (ppm) of dissolved solids and is considered to be of high quality if the total dissolved solids (TDS) are less than 600 ppm. It is not advised to regularly drink water with TDS levels more than 1000 ppm (WHO, 2017[27]).Desalination methods like reverse osmosis (RO), multi-stage flash (MSF), and multi-effect distillation (MED) have been widely used to produce drinking water, particularly in the Middle East and Australia (Ghaffour et al., 2013[14]; Elimelech and Phillip, 2011[11]). However, most desalination technologies have a high specific energy consumption, and only RO needs 3–10 kWh/m^3. Also, conventional dependence on fossil fuels to operate desalination units creates issues with emissions and sustainability (Elimelech and Phillip, 2011[11]; Cruz, 2008[8]). The environmental and economic effects of desalination using fossil fuels continue to be a major problem, despite developments in membrane technology, according to recent studies (Charcosset, 2009[5]; Morillo et al., 2014[26]; Zubair, 2023[44]).

Alternatives like wave energy and marine renewables are being studied. Waves offer reliable resources and a high energy density (2–3 kW/m wave front) in coastal zones (Cruz, 2008[8]). Over the past 40 years, a large number of experimental and demonstration projects have focused on wave-powered desalination. In projects like Carnegie's CETO (Australia) (Leijon and Bostrom, 2017[22]; Carnegie, 2015[23]), SAROS (US) (Yousri et al., 2023[40]; Saros, 2016[10]), and the NREL HERO-WEC (US) (Jenne et al., 2024[19]), point absorbers or surge devices are utilized to power RO units electrically or mechanically. The DELBUOY project (Hicks et al., 1989[18]), Odyssée (Lavars, 2014[21]; Project Odyssee, 2014[29]), and Vizhinjam OWCRO (Sharmila et al., 2004[31]) are a few other projects that have shown that integrating wave energy converters (WECs) with RO desalination is technically feasible. These studies show how various technologies are available, such as direct mechanical and hydraulic coupling, and highlight how important system integration and local resource assessment are for a successfull implementation.

These initiatives show the need for greater reliability and system-level optimization even though they have shown technological viability. Strong control strategies, hybridization with storage, and extensive modeling are crucial for real-world application because of the intermittent and varying nature of wave energy, which makes steady RO operation difficult (Suchithra et al., 2022[32]); Cheddie et al., 2010[6]). The ecological footprint of wave-powered systems can be reduced with proper placement and brine management, according to environmental impact studies (Folley and Whittaker, 2009[12]; Corsini et al., 2015[7]). The current state of development has been studied for multiple wave powered desalination devices utilizing various literatures available and presented in Table 1.1.

Table 1.1: How far the WEC/DES projects have proceeded and whether they are seemingly ongoing [22][4][19]

Concept	WEC/DES	Research	Simulation	Test	Deployed	Company	Ongoing
3D & surge	WABRO	x	x			x	
AaltoRO	WABRO	x	x				
Buoy array	WABRO	x	x				
CETO	WABRO	x	x	x	x	x	
Delbuoy	WABRO	x	x	x	x		
DEIM	WABRO	x	x				
Duck	WABVC	x	x				
ISWEC	WABRO	x	x				
Odyssée	WABRO	x	x		x		x
Oyster	WABRO	x	x				
SAROS	WABRO	x	x	x	x	x	x
Uppsala	WABRO	x					x
Vizhinjam	OWCRO	x	x	x	x		
WaveCatcher	OWCRO	x		x			
Wind/wave	WABRO	x					
HERO-WEC	WABRO	x	x	x	x		x

Where,

- **WEC/DES:** Wave Energy Converter integrated with Desalination unit
- **WABRO:** Wave Activated Body integrated with Reverse Osmosis
- **WABVC:** Wave Activated Body integrated with Vapor Compression
- **OWCRO:** Oscillating Water Column integrated with Reverse Osmosis

Point absorbers and surge devices are two of the more advanced WEC types. The efficiency of point absorbers is significantly reduced under low wave circumstances, despite the fact that they can be tuned for resonance with dominant sea states to convert vertical (heave) motion into mechanical or electrical energy (Babarit, 2016[2]; Cruz, 2008[8]). By using the energy of a flap or paddle's back-and-forth (surge) movement, surge devices like OSWEC, which are generally deployed in shallow water, can operate efficiently in a greater range of sea conditions (Babarit, 2016[2]; Leijon and Bostrom, 2017[22]). The choice between heave and surge is greatly affected by the local wave climate and site bathymetry; recent comparison studies (Giorgi and Ringwood, 2018[15]) have shown different efficiency characteristics and hydrodynamic responses.

By removing electrical conversion losses, direct mechanical connection to RO systems increases efficiency in off-grid situations (Lotfy et al., 2022[24]; Panzarella et al., 2024[28]). Approaches to mechanical and hydraulic connection, such the Odyssée system (Lavars, 2014[21]) and the AaltoRO project (Ylänen and Lampinen, 2014[39]), are becoming more popular as practical alternatives for remote areas.

For the optimization, scalability, and implementation of coupled WEC-RO desalination, it is now acknowledged that reliable numerical modeling, using time-domain, frequency-domain, and coupled modeling approaches is important (Yu and Jenne, 2018[42]; Zubair et al., 2023[44]).

1.2. Problem Statement

Wave-powered desalination continues to be uncommon on a big scale, even after technological advancements. The challenges are the very unpredictable and irregular character of ocean wave resources, which makes it more difficult to provide RO units with stable energy delivery (Ghaffour et al., 2013[14]; Rusu et al., 2021[30]). In actual offshore conditions, where both wave height and period fluctuate frequently, devices designed for a single design wave climate may not operate at their actual potential (Babarit, 2016[2]). Point absorbers such as RM3, are very effective at resonance but operate poorly outside of small optimum regions (Babarit, 2016[2]). Even though they are more adaptable, surge devices like OSWECs still need accurate tuning in order to manage storm loads and remain effective (Leijon and Bostrom, 2017[22]).

Complexity is increased when WECs are used with RO desalination. Wave-driven systems naturally provide variable, fluctuating energy, whereas RO membranes need high, steady pressure and are vulnerable to fouling and pressure changes (Elimelech and Phillip, 2011[11]). Real deployment issues, including fouling, device fatigue, brine disposal, and ecological effects, are frequently overlooked in numerical studies, which typically assume idealized wave inputs, simplified device hydrodynamics, and continuous water quality (Ghaffour et al., 2013[14]). Using time-domain simulation and an extensive matrix of sea states, this thesis addresses an important challenge of providing a comparative analysis of which WEC-RO configurations provide the best balance between Specific Energy Consumption (SEC), freshwater production, and operational stability under varying wave conditions.

1.3. Research Objective

This section provides the research questions that direct the study as well as an overview of the main research goal. Based on the gaps and difficulties found in the existing literature on wave-powered desalination and the integration of wave energy converters (WECs) with reverse osmosis (RO) desalination systems, the objective and questions have been developed.

The primary goal of this study is to simulate and contrast the performance of an oscillating surge wave energy converter (OSWEC) and a heaving point absorber (RM3) that are both directly connected to a reverse osmosis desalination subsystem under a realistic range of representative North Sea wave conditions. The main goals are to measure and compare their average water production and Specific Energy Consumption (SEC) and understand how each device reacts to varying sea conditions. With applications for sustainable freshwater production in coastal locations, the study aims to suggest which WEC-RO combination provides the most reliable and energy-efficient desalination performance (Ghaffour et al., 2013[14]; Rusu et al., 2021[30]).

This aim is to address a substantial knowledge gap in the comparative assessment of various wave-powered desalination technologies under practical operating conditions and responds to the growing demand for environmentally sustainable water resources (Elimelech and Phillip, 2011[11]).

1.3.1. Research Questions

This thesis aims to address the following important research questions in order to fulfill the previously stated objective:

- In a matrix of significant wave heights and energy periods typical of North Sea circumstances, how do the SEC and water production of the RM3 heaving point absorber and the OSWEC oscillating surge device compare when each is connected to a direct-drive reverse osmosis subsystem?
- Which device is more adaptable to sea state variability, and how do changes in significant wave height (Hs) and energy period (Te) affect each WEC-RO system's performance and operational stability?
- What are the advantages and limitations of simulating the dynamic behavior of coupled WEC-RO systems using a time-domain numerical method that uses hydraulic coupling and hydrodynamic coefficients derived from boundary element method-based solvers?
- What recommendations, in the context of the comparative findings and observed patterns, may be made to enhance WEC-RO design, modeling, and deployment?

1.4. Scope

Two well-defined Wave Energy Converters, RM3 (Heaving device) and OSWEC (Surging device), each connected to a hydraulically powered RO subsystem, are modeled in this strictly numerical thesis. The study:

- Captures relevant device dynamics, including fluid memory, by using time-domain simulations with hydrodynamic data from linear frequency domain Boundary Element Method solvers based on the linear potential flow theory.
- Uses velocity input from the Wave Energy Converter and adjust it to simulate mechanical-to-hydraulic energy conversion in a hydraulic piston and Reverse Osmosis model (Yu et al., 2017[41])
- Combines five wave heights (1–5 m) and five energy periods (5–9 s) that are typical for the North Sea to simulate 25 sea states.
- Builds matrices for SEC, water production, and permeate concentration by automating the parameter analysis using the Multiple Condition Run (MCR) module.
- Highlights the possibility to interpolate performance for any given sea state, steady-state freshwater output, and energy efficiency of the system.

The thorough resource evaluation of the North Sea provided by (Beels et al., 2007[3]) significantly influenced the selection of sea states for this thesis. The majority of observed conditions are concentrated between significant wave heights of 1 to 5 meters and energy periods of 5 to 9 seconds, according to their analysis of wave data from several North Sea locations, including the Belgian, Dutch, German, Danish, Norwegian, and UK continental shelves. For example, the characteristic sea state at Ekofisk (central North Sea) is Hs=2.2 m and Te=6.3 s, but it is roughly Hs=1.2 m and Te=5.1 s along the Belgian shelf. The characteristic sea state increases to Hs=2.7 m Te=7.5 s at the more active northern region of Haltenbanken (Norwegian shelf). The thesis makes sure that the simulation matrix accurately covers the most common and important sea states for WEC devices in the North Sea by using these ranges. According to (Beels et al., 2007[3]), this supports the selection as being both representative of the area and essential for understanding device performance and operability under normal deployment conditions.

By applying the solution-diffusion model for reverse osmosis to determine the salinity of the desalinated water, this thesis provides a clear check on the quality of the permeate water (Leijon and Bostrom, 2017[22];Chakravarthi et al., 2024[4]). The model confirms whether the permeate satisfies recognized standards for potable water (usually <600 ppm) (WHO, 2017[27]), although the primary focus is still on comparing the specific energy consumption and water production rates of the desalination systems across the sea states.

Detailed environmental effect studies, experimental validation, and cost analyses are not included. Although not specifically modeled, long-term impacts including fouling, system degradation, or economic scaling have been noted (Ghaffour et al., 2013[14]; Elimelech and Phillip, 2011[11]).

The linearized time-domain hydrodynamic method is the basis of this thesis. It uses linear potential flow theory[1][20], which is used in Boundary Element Method (BEM) solvers, to obtain all hydrodynamic parameters, including added mass, radiation damping, and wave excitation forces. The time-domain characteristics of the wave energy converters are then modeled using these coefficients in a commercial tool to simulate the behaviour of the devices.

1.5. Approach

- Two WEC-RO systems were chosen for comparison based on a review of the literature to find research gaps in wave-powered desalination (Ghaffour et al., 2013[14]; Elimelech and Phillip, 2011[11]; Babarit, 2015[2]).
- Establish the goals of the study and choose two typical devices: an oscillating surge WEC and a heaving point absorber (Leijon and Bostrom, 2018[22]; Lotfy et al., 2022[24]).
- Utilizing validated geometries, model the hydrodynamics of the device and use a BEM solver to extract frequency-domain coefficients (Cruz, 2008[8]).
- Use the convolution integral for radiation forces to simulate a coupled system in the time domain (Babarit, 2015[2]). For realistic feedback, use of Simulink to design the hydraulic subsystem (Yu et al., 2018[42]).
- Run simulations up to 1000 s for 25 distinct sea states (combinations of Hs and Te), averaging the results throughout the 500–1000 s steady-state interval.
- Calculate metrics for performance using post-process outputs, such as average specific energy consumption (SEC), average water production per day, and permeate salinity and display the results as heatmaps and power matrices.
- Quantitatively compare device performance and discuss the results in the context of real-world deployment, limitations, and suggestions for further study.

1.6. Thesis Structure

Chapter 1: Introduction The history of water scarcity worldwide and the demand for sustainable desalination methods are covered in this chapter. It outlines the study's scope and approach, defines the problem statement, and develops the primary research goal and research questions. An outline of the thesis structure concludes the chapter.

Chapter 2: Methodology The numerical modeling framework employed in this study is described in the second chapter. The numerical modeling of the two wave energy converter (WEC) types—the oscillating surge device (OSWEC) and the heaving point absorber (RM3) is explained first. The reverse osmosis (RO) desalination subsystem's modeling is then described in detail. The coupling of each WEC device with the RO desalination unit is further explained in this chapter, along with the transfer and use of simulation data. The full simulation setup, including the choice of sea states and the calculation processes for time-domain simulations, is presented in the last section.

Chapter 3: Results and Discussions The simulation results are presented and examined in this chapter. It begins with detailed results for the oscillating surge WEC desalination system and the heaving point absorber under specific sea state parameters. The power matrices for specific energy consumption and average water output for each of the sea states under study are included in the comparative analysis that follows. The interpolation technique used to estimate performance at any desired sea state within the measured range is also explained in this chapter. The results are interpreted, the approach's assumptions and limitations are discussed, and suggestions and future study directions are provided in the discussion section.

Chapter 4: Conclusion The key findings are compiled in the last chapter, which also makes clear conclusions regarding the relative effectiveness of the two WEC devices for wave-powered desalination. In addition, the chapter considers the research issues, discusses the results applications, and suggests possible directions for further research.

2

Methodology

2.1. Numerical Modeling of the Wave Energy Converter

Wave energy converters (WECs) can be modeled by numerically solving algebraic and ordinary differential equations that characterize how the device interacts with ocean waves. For this kind of research, MATLAB/Simulink[36] based open-source program WEC-Sim [34] offers a stable environment along with the MATLAB[36] add-ons like Simscape, Simscape Driveline, Simscape Fluids, and Simscape Multibody. The capacity of WEC-Sim to accurately represent dynamic interactions between wave energy devices and marine environments makes it extremely helpful.

Taking into consideration the full dynamic response of WECs, the numerical modeling procedure in WEC-Sim mainly solves the equations of motion in the time domain, which is the Cummins equation (Cummins, 1962[9]). Transient and nonlinear phenomena that normally occur in actual sea conditions are captured in the time domain. Understanding how wave devices react to wave forces, motions, and power harnessing devices is particularly advantageous.

Several different forces acting simultaneously are incorporated into the basic equation that WEC-Sim uses to describe device motions. The expression for this governing equation of motion in a particular Degree Of Freedom (DOF) is

$$m\ddot{x}(t) + A_\infty \ddot{x}(t) + \int_0^t K(t-\tau)\dot{x}(\tau)\,d\tau + Cx(t) = F_{\text{ext}}(t) \tag{2.1}$$

- m - Mass of the body
- A_∞ - Added mass at infinite frequency for a particular DOF
- $\ddot{x}(t)$ - Acceleration of the body at time t for a particular DOF
- $K(t-\tau)$ - Radiation impulse response function (memory kernel) for a particular DOF
- $\dot{x}(\tau)$ - Velocity of the body at time τ for a particular DOF
- C - Hydrostatic restoring coefficient for a particular DOF
- $x(t)$ - Displacement of the body at time t for a particular DOF
- $F_{\text{ext}}(t)$ - Total external force (e.g., wave excitation force) at time t

WEC-Sim [34] requires users to provide accurate hydrodynamic parameters before it can run. These parameters consist of the impulse response functions, wave excitation coefficients, radiation damping, and the added mass. Frequency-domain solvers such as the Boundary Element Method (BEM) solver WAMIT[37] are commonly used to compute these values. The frequency-domain data from WAMIT is processed and constructed using state-space approximation that WEC-Sim can use for its time-domain simulations using a specially developed program called BEMIO[33].

The OSWEC, an oscillating surge device, and the RM3, a heaving two-body point absorber, are two frequently used WEC models in WEC-Sim. Because of their verified hydrodynamic properties and well-documented geometries, these models are used as benchmark configurations in many different research projects. These models' pre-calculated parameters from available sources guarantee that WEC-Sim simulations can correctly simulate device responses and performance attributes. By precisely integrating a variety of forces and dynamic effects, WEC-Sim's strong framework enables thorough modeling of wave energy converters and provides accurate insights into WEC behavior under varied offshore conditions.

2.1.1. Heaving WEC Device

In this study, the RM3 example from WEC-Sim, modified for site-specific conditions, is used to represent the heaving point absorber device. The upper float of the two-body axisymmetric point absorber RM3 travels in heave in relation to a submerged spar. The rm3.out file was modified to reflect a water depth of 200 meters in order to adapt the hydrodynamic data from the WAMIT frequency-domain solver to appropriately match real-world deployment. Since raising the depth from infinite to 200 meters has no effect on RM3 hydrodynamics for the majority of operating sea states, this depth was chosen as a practical value and also to incorporate the mooring cables, which are designed for the same water depth in WEC-Sim applications repository[35].

This study's RM3 device is a traditional two-body axisymmetric point absorber that has a submerged cylindrical spar and a floating cylindrical buoy. The spar beneath the float is 30 m in diameter, 38 m in height. The float itself is 20 m in diameter, 5 m in height as interpreted with BEMRosetta[43] and a simple vizualisation can be seen in Figure 2.1 with details in Table 2.1. The two bodies are free to move in relation to one another along the vertical axis (heave motion) despite being joined by a stiff connection. The spar, which has more mass and drag, acts as a reference structure to improve relative motion and energy capture, while the float moves up and down in response to incoming waves. With the float moving with the waves and the spar attached to the bottom by a mooring mechanism, this configuration only actively models the vertical (heave) degree of freedom for energy extraction. This arrangement makes it possible for the linked desalination unit to receive mechanical power and absorb wave energy efficiently. The geometry, including meshing and defined normal vectors as visualized with BEMRosetta[43], can be seen in Figure 2.2.

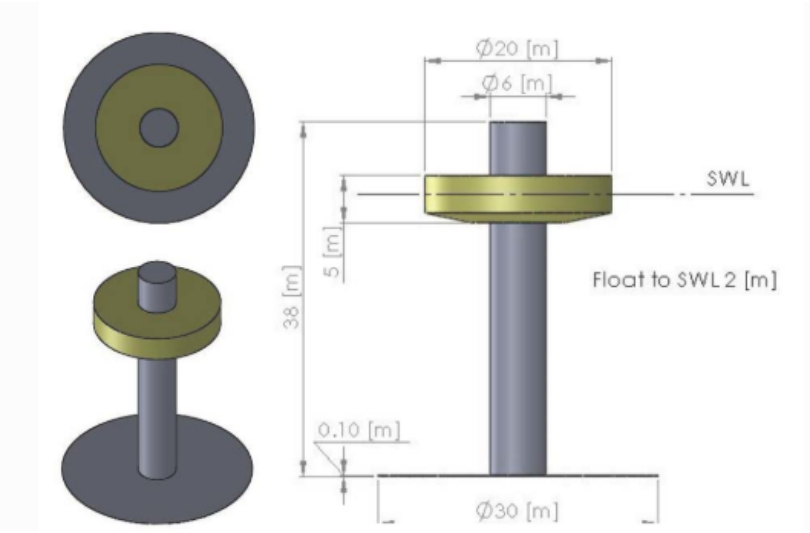

Figure 2.1: Geometry description for Heaving RM3 Device [34]

Table 2.1: Main Characteristics of the RM3 Heaving Device

Parameter	Float	Spar
Diameter [m]	20	6
Height [m]	5	38
Mass [tonne]	727.01	878.30
Material	Steel	Steel

The simulation uses a mooring package from the WEC-Sim Applications GitHub repository[35] that is intended for the same 200-meter water depth in order to ensure realistic mooring dynamics. In order to incorporate mooring effects, the Simulink model is modified to incorporate the mooring matrix into the equations of motion. MoorDyn[16], an open-source dynamic mooring line model, has been integrated with WEC-Sim to improve physical accuracy. The MinGW-w64 C/C++/Fortran compiler in MATLAB is used in the MoorDyn integration, allowing for real-time mooring force calculation as the device interacts with waves.

The core time-domain equation (Journee and Massie, 2001[20]) of motion for the heaving float and the heaving spar is:

$$m_1\ddot{x}_1(t) = F_{\text{hydro,1}}(t) + F_{\text{coupling}}(t) + F_{\text{rest,1}}(t) \tag{2.2}$$

$$m_2\ddot{x}_2(t) = F_{\text{hydro,2}}(t) + F_{\text{coupling}}(t) + F_{\text{moor,2}}(t) + F_{\text{rest,2}}(t) \tag{2.3}$$

where

- m_1 is the mass of the float,
- m_2 is the mass of the spar,
- $\ddot{x}_1(t)$ is the vertical acceleration of the float relative to the fixed (global) frame,
- $\ddot{x}_2(t)$ is the vertical acceleration of the spar relative to the fixed frame,
- $F_{\text{hydro,1}}(t)$ is the total hydrodynamic force on the float,
- $F_{\text{hydro,2}}(t)$ is the total hydrodynamic force on the spar,
- $F_{\text{coupling}}(t)$ is the coupling force, which is a feedback from the reverse osmosis system and introduces a resistance to the motion, acting oppositely on the float and spar,
- $F_{\text{moor,2}}(t)$ is the mooring force on the spar (from MoorDyn[16]),
- $F_{\text{rest,1}}(t)$ is the hydrostatic restoring force on the float,
- $F_{\text{rest,2}}(t)$ is the hydrostatic restoring force on the spar.

Relative motion and the coupling force depend on the relative velocity and displacement between the float and spar:

$$x_{\text{rel}}(t) = x_1(t) - x_2(t) \tag{2.4}$$

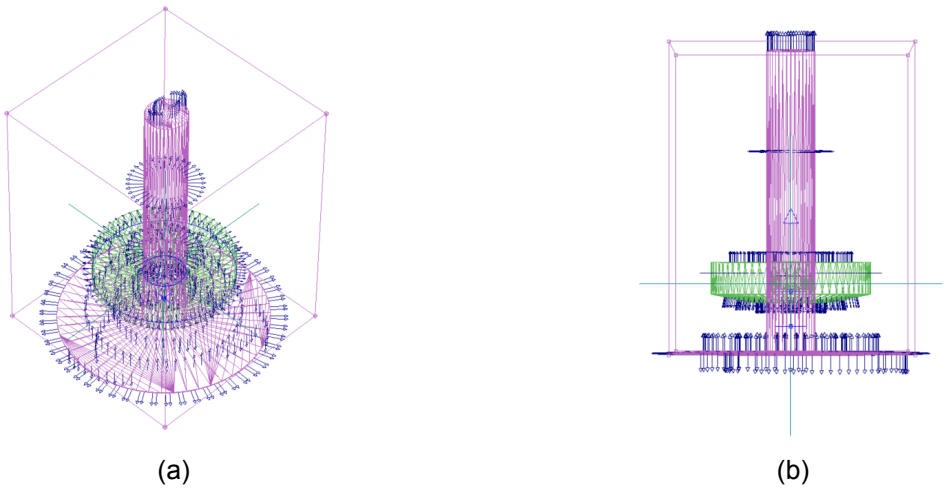

(a) (b)

Figure 2.2: Geometry with Meshing and Normal Vectors for RM3 (a) Isometric view (b) Side view

The modeling results fully represent the relative motion between the float and spar, which determines the PTO force and actual energy input to the desalination unit.

Since there is no linear generator in this application, the translational PTO damping is set to zero, but a coupling force is introduced here, which is the feedback force from the reverse osmosis subunit. Instead, the hydraulically powered reverse osmosis (RO) desalination component uses all of the absorbed energy taken as a velocity input generated by the WEC device. In order to prepare the simulation for a full energy interaction study later on, the Simulink model is further modified to output the relative WEC velocity and integrate with a piston and RO subsystem. The schematic model of the WEC, including mooring, can be observed in Figure 2.3.

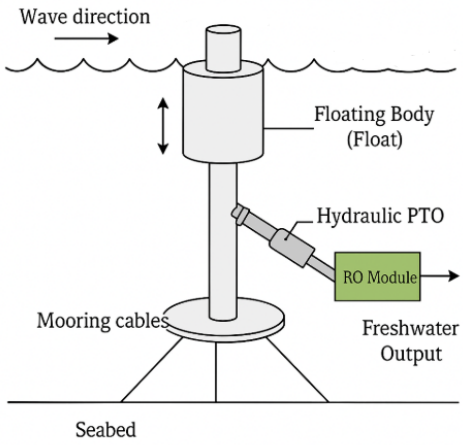

Figure 2.3: Schematic Diagram for RM3 Heaving device

The hydrodynamic parameters for the geometry as obtained using WAMIT are then approximated by state space approximation using BEMIO[33] and plotted against frequency for Heave direction in MATLAB as seen in Figures 2.4, 2.5, and 2.6 for the Normalized Added Mass, Normalized Radiation Damping and the Normalized Excitation Force Magnitude respectively.

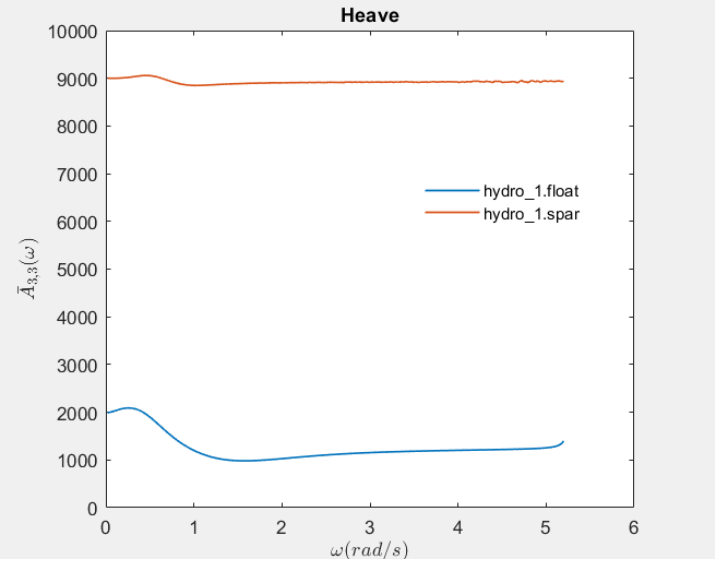

Figure 2.4: Normalized Added Mass against Frequency for RM3 Heaving WEC

The normalized added mass is defined as:

$$\bar{A}_{i,j}(\omega) = \frac{A_{i,j}(\omega)}{\rho} \tag{2.5}$$

Where,

- $\tilde{A}_{i,j}(\omega)$: Normalized added mass coefficient as a function of angular frequency ω.
- ρ: Fluid density.
- i: Degree of freedom (DOF) in which the force is considered (Heave in this case).
- j: Degree of freedom (DOF) in which the motion is considered.

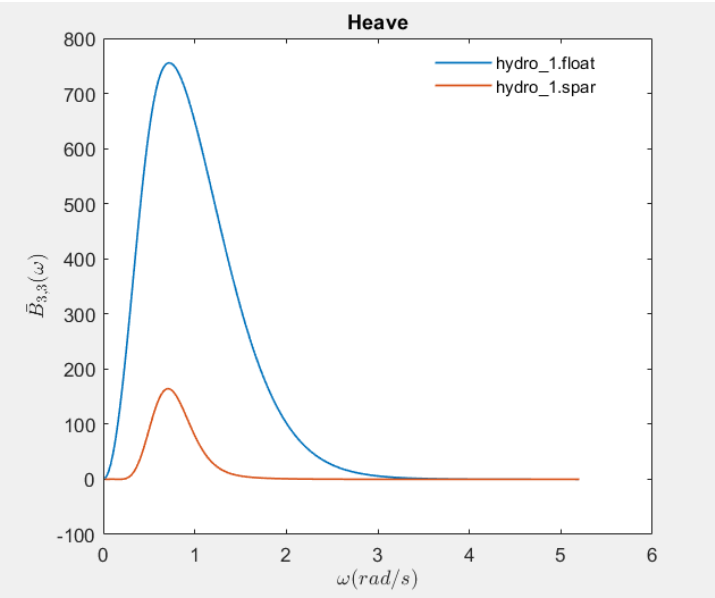

Figure 2.5: Normalized Radiation Damping against Frequency for RM3 Heaving WEC

The normalized radiation damping is defined as:

$$\bar{B}_{i,j}(\omega) = \frac{B_{i,j}(\omega)}{\rho\omega} \tag{2.6}$$

Where,

- $\tilde{B}_{i,j}(\omega)$: Normalized radiation damping coefficient as a function of angular frequency ω.
- ω: Frequency [rad/s].

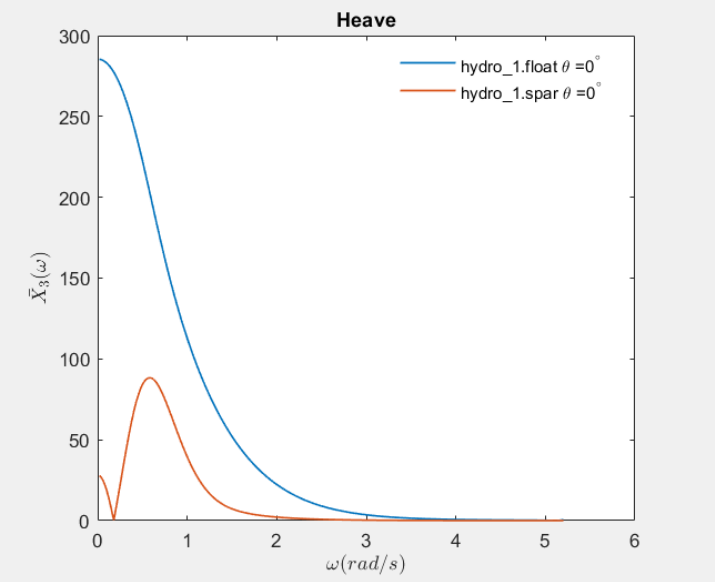

Figure 2.6: Normalized Excitation Force Magnitude against Frequency for RM3 Heaving WEC

The normalized excitation force magnitude is defined as:

$$\bar{X}_i(\omega, \theta) = \frac{X_i(\omega, \theta)}{\rho g} \tag{2.7}$$

- $\tilde{X}_i(\omega, \theta)$: Normalized excitation force magnitude for the i^{th} degree of freedom, as a function of angular frequency ω and incident wave angle θ.
- g: Gravitational acceleration.
- θ: Incident wave angle [degrees].
- i: Degree of freedom (DOF) under consideration (Heave in this case).

2.1.2. Oscillating Surge WEC Device

In this thesis, a flap-type device that transforms wave motion into mechanical power is represented using the Oscillating Surge Wave Energy Converter (OSWEC) example from the WEC-Sim repository. The OSWEC is a huge, rectangular flap that is anchored to the seabed and hinged at the base. Its dimensions are 18 m in width, 11.5 m in height out of which 10.9 m is submerged when stationary, and 1.8 m in thickness as obtained with BEMRosetta[43]. While the foundation itself stays fixed, the flap is free to revolve around it in the direction of the surge. The geometry parameters can be visualized in Figure 2.7 with details in Table 2.2.

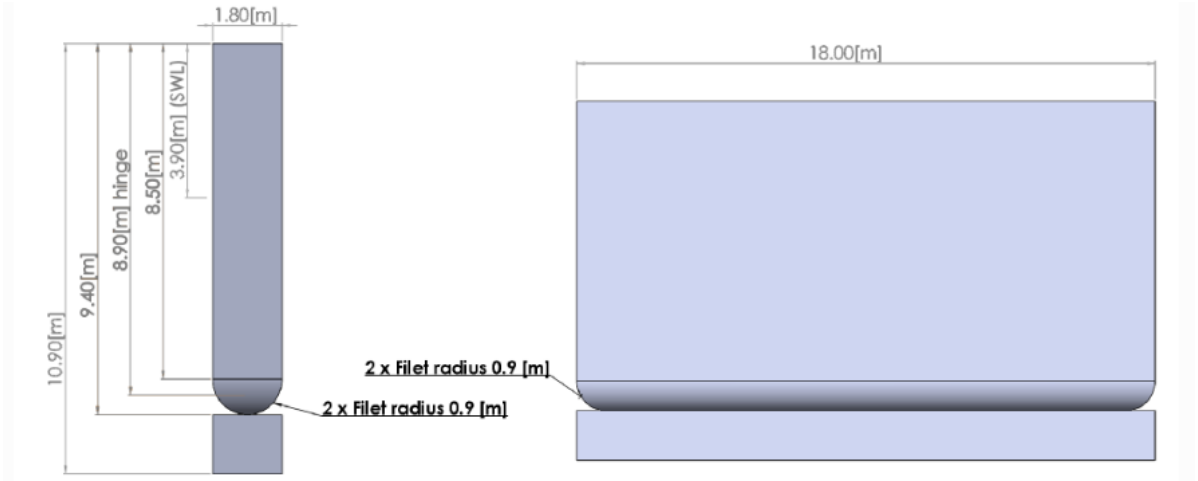

Figure 2.7: Geometry description for Oscillating OSWEC Device [34]

Table 2.2: Main geometric characteristics and mass of the OSWEC device

Parameter	Value	Unit
Flap height (vertical)	11.50	m
Flap width (horizontal)	1.80	m
Hinge depth below SWL	8.90	m
Distance from SWL to bottom	10.90	m
Flap span	18.00	m
Flap mass	127	tonne

Frequency-domain solver WAMIT[37] is used to calculate the hydrodynamic coefficients at a sea depth of 10.9 meters using the meshed geometry with defined normal vectors as visualized in Figure 2.8, including normalized added mass, radiation damping, and wave excitation forces and is then converted to a WEC-Sim compatible format with .h5 extension using BEMIO, as done for the RM3 device. Due to the OSWEC's nearshore deployment and direct attachment to the bottom, local bathymetry is essential for precise modeling, which makes this particular water depth significant. The detailed modeling is described in (Yu and Jenne,2017[41]) .

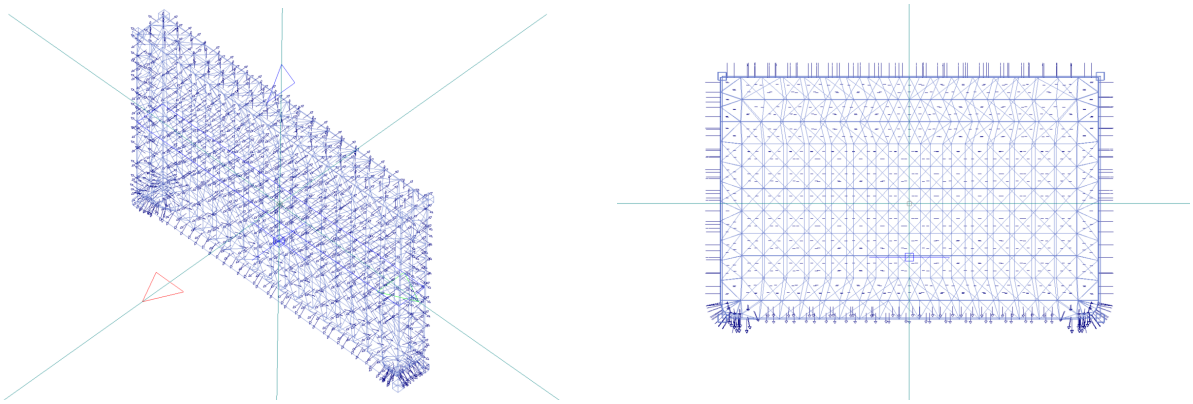

Figure 2.8: Geometry with Meshing and Normal Vectors for OSWEC (a) Isometric view (b) Front view

In the time domain, the equation (Journee and Massie, 2001[20]) of motion for the rotational movement of the OSWEC flap is expressed as:

$$I\,\ddot{\theta}(t) = M_{\text{exc}}(t) + M_{\text{rad}}(t) + M_{\text{coupling}}(t) + M_{\text{rest}}(t) \tag{2.8}$$

where

- I is the moment of inertia of the flap,
- $\ddot{\theta}(t)$ is the angular acceleration,
- $M_{\text{exc}}(t)$ is the wave excitation moment,
- $M_{\text{rad}}(t)$ is the radiation moment,
- $M_{\text{coupling}}(t)$ is the coupling moment which is the feedback from the RO subunit and provides resistance to the flap's rotational motion,
- $M_{\text{rest}}(t)$ is the hydrostatic restoring moment.

The flap's angular velocity, which is necessary for connection with the piston and Reverse Osmosis (RO) subsystem, is output by the Simulink model. Instead of converting the rotational energy into electrical power, the PTO is designed to capture it and send it straight to the desalination unit as velocity input. Through the incorporation of these adjustments, the model accurately depicts nearshore deployment and sets up the simulation for a thorough assessment of the OSWEC-powered desalination system's performance. The schematic figure of this device can be visualized in Figure 2.9.

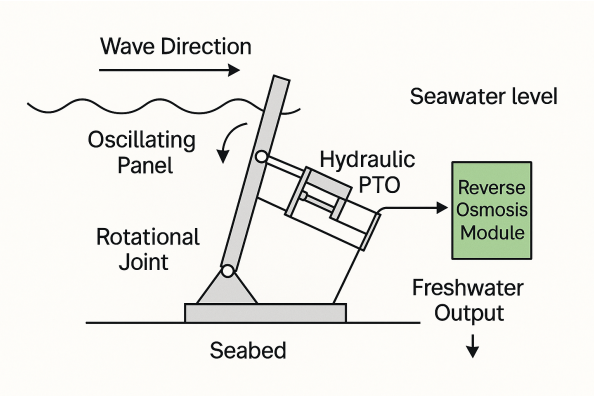

Figure 2.9: Schematic Diagram for OSWEC Heaving device

The hydrodynamic parameters are similarly constructed to a WEC-Sim compatible format using state-space approximation through BEMIO[33] and plotted for surge direction in MATLAB as shown in Fig-

ures 2.10, 2.11, and 2.12 for the Normalized Added Mass, Normalized Radiation Damping and the Normalized Excitation Force Magnitude respectively.

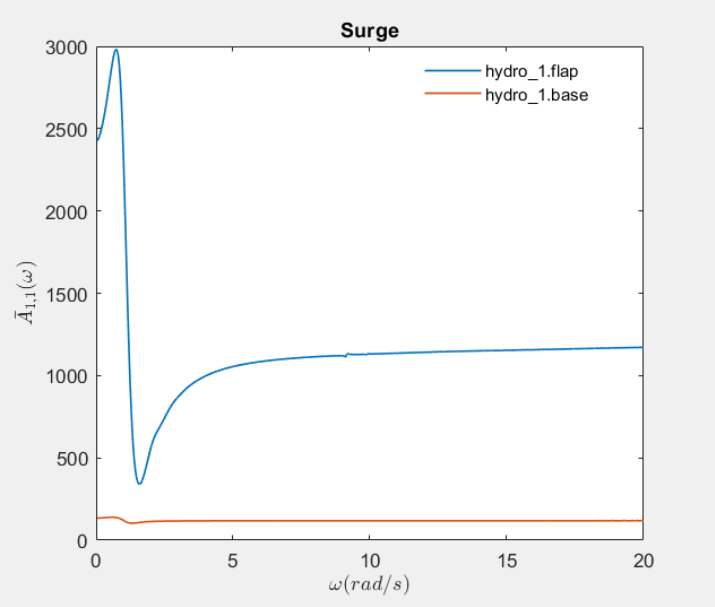

Figure 2.10: Normalized Added Mass against Frequency for OSWEC Surging WEC

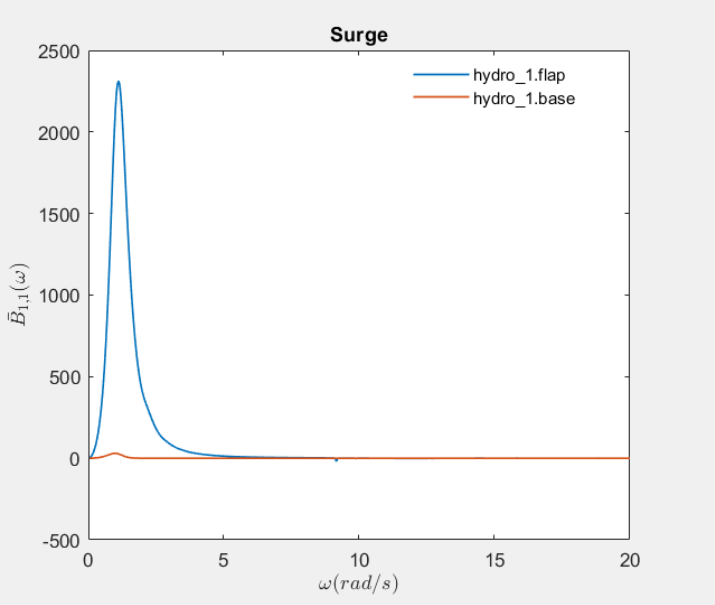

Figure 2.11: Normalized Radiation Damping against Frequency for OSWEC Surging WEC

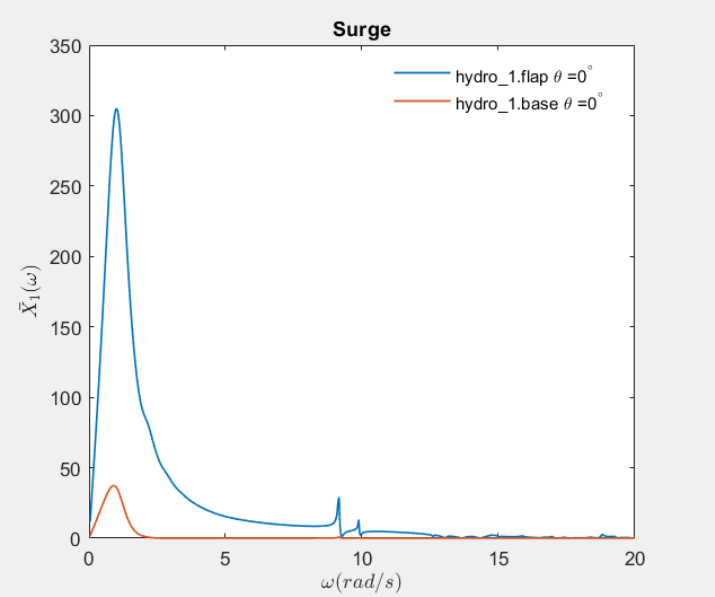

Figure 2.12: Normalized Excitation Force Magnitude against Frequency for OSWEC Surging WEC

2.2. Numerical Modeling of the Reverse Osmosis Desalination Unit

In accordance with the open-source design found in the WEC-Sim Applications GitHub repository[35], the reverse osmosis (RO) desalination unit modeled in this study makes use of a comprehensive hydraulic network. In order to separate freshwater (permeate) from concentrated brine, this subsystem transforms the mechanical power from the WEC into high-pressure hydraulic energy. This energy is then utilized to push seawater through a semi-permeable membrane, and a similar modeling technique has been implemented in (Suchithra et al.,2022[32]) and a same desalination unit has been used by (Yu et al., 2017[41]) for which the schematic visualization can be observed in Figure 2.13.

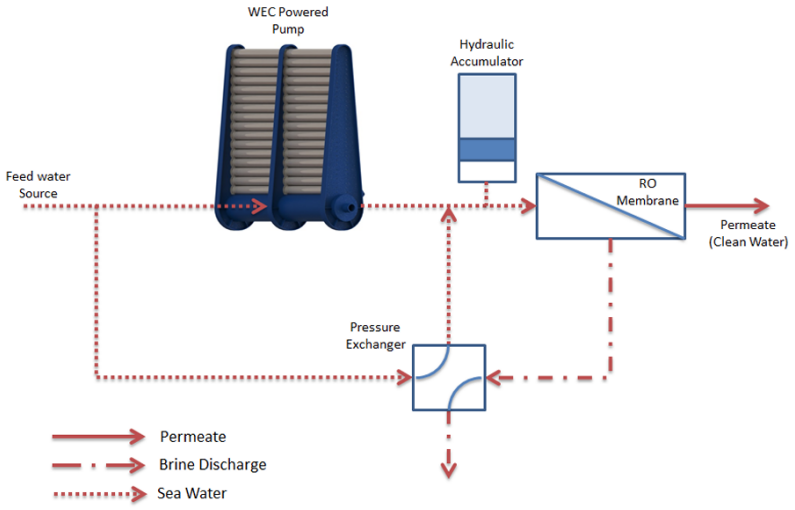

Figure 2.13: Schematic visualization of the WEC-powered RO Desalination Unit [41]

- **Input and Hydraulic Cylinder**

  Depending on the device, the WEC's motion can either rotate or heave, which provides velocity as input to the system's initial double-acting hydraulic cylinder. There are two chambers in the double-acting cylinder. In order to ensure essentially constant fluid movement and pressure for the remainder of the system, the cylinder converts the mechanical movement of the WEC into pressurized hydraulic flow in both directions (Folley et al.,2008[13]).

  Operating Principle:

  A piston separates the two hydraulic chambers (A and B) that make up the cylinder. The piston rod can move in both directions when there is pressurized fluid in either chamber.

  Numerical Modelling and Equations:

  The following is the basic relationship that governs the force balance in the double-acting cylinder:

$$F_{\text{hydraulic}} = P_A A_A - P_B A_B \tag{2.9}$$

  where:

  - $F_{\text{hydraulic}}$: Force exerted by the cylinder piston (N).
  - P_A: Pressure in chamber A located on one end of the piston inside the cylinder (Pa).
  - A_A: Piston area in chamber A (m^2).
  - P_B: Pressure in chamber B located on the other end of the piston inside the cylinder (Pa).
  - A_B: Piston area in chamber B (m^2).

  Flow Rate Relationships:

  The piston areas and piston velocity have a direct relationship with the volumetric flow rates in the hydraulic cylinder chambers, which are determined by:

$$Q_A = v \cdot A_A \tag{2.10}$$
$$Q_B = v \cdot A_B \tag{2.11}$$

  where:

  - Q_A is the volumetric flow rate in chamber A ($\text{m}^3\,\text{s}^{-1}$),
  - Q_B is the volumetric flow rate in chamber B ($\text{m}^3\,\text{s}^{-1}$),
  - v is the piston velocity ($\text{m}\,\text{s}^{-1}$).

  The hydraulic power transfer from the WEC to the reverse osmosis (RO) subsystem is controlled by these flow rates.

  Numerical implementations of fully inelastic hard-stops with high stiffness (penetration coefficient) are used to implement the physical constraints at the piston stroke boundaries. These limitations, which are mathematically defined as follows, prevent penetration beyond physical bounds:

$$F_{\text{hard-stop}} = k_{\text{pen}} \cdot x_{\text{pen}} \tag{2.12}$$

  where:

  - $F_{\text{hard-stop}}$: Hard-stop reaction force (N).
  - k_{pen}: Penetration coefficient (stiffness coefficient), $(\text{s} \cdot \text{N}/\text{m}^2)$.
  - x_{pen}: Penetration distance beyond the stroke limit (m).

Model Parameters:

Below is a summary of the numerical parameters used in this Simulink model:

Table 2.3: Double-Acting Hydraulic Cylinder Parameter [35]

Parameter	Value	Unit
Piston area A	0.26	m^2
Piston area B	0.26	m^2
Piston stroke	12	m
Piston initial distance from cap A	6	m
Penetration coefficient	1×10^{12}	s·N/m^2

- **Accumulator**

In the Simulink model, the Gas-Charged Accumulator serves as a hydraulic energy storage device. When power input is at its highest, it stores hydraulic energy, which is then released when power is at its lowest. The accumulator is made up of two chambers: a fluid chamber and a gas chamber, which are divided by a flexible component (such as a bladder, diaphragm, or piston).

Operating Principle:

The accumulator is made up of two separate chambers that are divided by a flexible interface, like a bladder, diaphragm, or piston:

- **Gas Chamber:** Packed with a precharged gas, typically nitrogen or air.
- **Fluid Chamber:** The hydraulic system is directly connected to this.

Hydraulic fluid stores hydraulic energy by compressing the gas as it enters the fluid chamber. On the other hand, the compressed gas expands when hydraulic pressure drops, pushing fluid out and reintroducing stored energy into the system.

The equation that describes the polytropic process of fluid-gas interaction inside the accumulator(Folley et al.,2008[13]) is shown:

$$PV^n = \text{constant} \tag{2.13}$$

where:

- P: Absolute gas pressure in the chamber (Pa).
- V: Gas volume in the chamber (m^3).
- n: Polytropic exponent (specific heat ratio; typically $n = 1.4$ for air).

Therefore, the following is an equation for the instantaneous gas chamber pressure:

$$P = P_0 \left(\frac{V_0}{V} \right)^n \tag{2.14}$$

where:

- P_0: Initial precharge gas pressure (Pa).
- V_0: Initial gas chamber volume (m^3).
- V: Instantaneous gas chamber volume (total volume minus fluid chamber volume) (m^3).

Mechanical Constraints:

In order to avoid unrealistic conditions, the accumulator model also includes mechanical hard-stop limitations, particularly:

- **Minimum Gas Volume Constraint:** Ensures that the gas chamber never fully collapses.
- **Hard-stop Stiffness and Damping:** Activated to maintain physical accuracy and numerical stability when the separator reaches volume ends.

Model Parameters:

The numerical values of the parameters used in the model are summarized below:

Table 2.4: Gas-Charged Accumulator Parameters[35]

Parameter	Value	Unit
Total accumulator volume	4	m^3
Minimum gas volume	4×10^{-5}	m^3
Precharge pressure (gauge)	3.0×10^6	Pa
Specific heat ratio	1.4	–
Hard-stop stiffness coefficient	1×10^7	Pa/m^3
Hard-stop damping coefficient	1×10^7	$s{\cdot}Pa/m^6$

- **Pressure Relief Valve and Hydraulic Sensors**

The Simulink model's Pressure Relief Valve works as a safety feature to keep the hydraulic system pressure within specified limits. A data sheet-based linear relationship between the opening area and pressure is used to represent this valve.

Operating Principle:

As long as the pressure at the valve inlet stays below the set valve pressure, the valve stays completely closed. The control part of the valve raises from its position to allow fluid to flow from the inlet to the outlet when the inlet pressure exceeds the set limit. The system pressure is then decreased by directing extra hydraulic fluid, generally back to a outlet as visualized in Appendix C Figure C.4.

- The valve opening area gradually grows until it reaches its maximum area if the flow discharge is insufficient and the pressure keeps rising.

Numerical Modelling and Equations:

A linear relationship between the valve opening area and the inlet pressure is used in the numerical modeling:

$$A_{\text{valve}} = \begin{cases} A_{\text{inital}}, & P_{\text{inlet}} < P_{\text{set}} \\ \text{Linear function of } (P_{\text{inlet}} - P_{\text{set}}), & P_{\text{set}} \leq P_{\text{inlet}} \leq (P_{\text{set}} + P_{\text{range}}) \\ A_{\text{max}}, & P_{\text{inlet}} > (P_{\text{set}} + P_{\text{range}}) \end{cases} \tag{2.15}$$

where:

- A_{valve}: Valve passage area (m^2).
- A_{initial}: Initial Valve passage area (m^2).
- A_{max}: Maximum valve passage area (m^2).
- P_{inlet}: Inlet pressure (Pa).
- P_{set}: Valve preset opening pressure (Pa).
- P_{range}: Valve regulation pressure range (Pa).

The discharge coefficient C_d, is taken into account when calculating the hydraulic fluid flow through the valve using orifice equations:

$$Q = C_d A_{\text{valve}} \sqrt{\frac{2\Delta P}{\rho}} \tag{2.16}$$

where:

- Q: Volumetric flow rate (m^3/s).
- C_d: Flow discharge coefficient.
- ΔP: Pressure differential across valve (Pa).
- ρ: Fluid density (kg/m^3).

Model Parameters:

The following table provides a summary of the numerical parameters used in this Simulink model:

Table 2.5: Pressure Relief Valve Parameters [35]

Parameter	Value	Unit
Maximum passage area	2.67×10^{-2}	m^2
Valve pressure setting	5.6×10^{6}	Pa
Valve regulation range	1×10^{5}	Pa
Flow discharge coefficient	0.7	–
Initial area	1×10^{-12}	m^2

- **Pressure Exchanger**

The pressure exchanger is a crucial component for efficiency. Before it reaches the RO membrane, this component recovers energy from the high-pressure brine (waste) stream and transfers it to the incoming seawater stream. The system's efficiency is increased by exchanging pressure, which lowers overall energy usage and can reduce the SEC from 6-8 kWh/m^3 to 4-5 kWh/m^3 as stated in (Malaeb et al.,2011[25]).

Subsystem Components and Operation:

The subsystem for the pressure exchanger is made up of:

- **Fixed-Displacement Pump**: Mechanically transmits hydraulic energy from the hydraulic motor shaft to seawater.
- **Hydraulic Motor**: Transforms high-pressure brine's hydraulic energy into mechanical rotational energy.
- **Linear Hydraulic Resistance**: Represents the hydraulic resistance that occurs when seawater passes through the system.
- **Hydraulic Flow Rate Sensors**: Measure the subsystem's flow rates..

Numerical Modelling and Equations:

Fixed-Displacement Pump and Hydraulic Motor:

Volumetric displacement principles govern the operation of both pump and motor:

$$Q = D \cdot \omega \tag{2.17}$$

$$T = D \cdot \Delta P \tag{2.18}$$

where:

- Q: Volumetric flow rate (m^3/s).
- D: Displacement (m^3/rad).
- ω: Angular velocity (rad/s).
- T: Torque (N·m).
- ΔP: Pressure difference across device (Pa).

Linear Hydraulic Resistance:

Proportional relationship is followed by the linear hydraulic resistance:

$$\Delta P = R_h \cdot Q \tag{2.19}$$

where:

- ΔP: Pressure difference across the resistance (Pa).
- R_h: Hydraulic resistance ($Pa/(m^3/s)$).
- Q: Flow rate through resistance (m^3/s).

Subsystem Parameters:

The numerical values of the parameters used in the model are summarized below:

Table 2.6: Fixed-Displacement Pump and Hydraulic Motor Parameters [35]

Parameter	Value	Unit
Displacement	4.75×10^{-6}	m^3/rad
Nominal shaft angular velocity	188	rad/s
Nominal pressure gain	100×10^5	Pa

Table 2.7: Linear Hydraulic Resistance Parameter [35]

Parameter	Value	Unit
Resistance (R_h)	2.7377×10^6	Pa/(m^3/s)

- **RO Membrane Subsystem**

  The main component of desalination is the RO membrane. When pressurized seawater reaches the membrane module, water molecules flow across it, leaving behind brine, which is made up of dissolved salts and other impurities (Folley et al.,2008[13]; Zubair, 2023[44]).

  The reverse osmosis (RO) process was simulated in this thesis using a solution-diffusion model. The net driving pressure, which is the difference between the predefined osmotic pressure ($\Delta\pi$) which is the minimum pressure for the diffusion to occur and the applied hydraulic pressure (Δp), controls the water flux over the membrane. This is how the permeate flow rate (Q_p) is computed:

$$Q_p = A_\omega A_m(\Delta p - \Delta\pi) \tag{2.20}$$

  where

  - A_ω is the water permeability coefficient (m/s/bar),
  - A_m is the membrane active surface area (m^2),
  - Δp is the hydraulic pressure difference across the membrane (bar),
  - $\Delta\pi$ is the osmotic pressure difference (bar).

  The following is used to estimate the solute concentration (C_p) in the permeate:

$$C_p = \frac{C_m}{\frac{A_\omega}{B_s}(\Delta p - \Delta\pi) + 1} \tag{2.21}$$

  where

  - C_m is the feed (seawater) salt concentration (ppm),
  - B_s is the salt permeability coefficient (m/s),

  The Reverse Osmosis (RO) membrane subsystem implemented in the Simulink model simulates the separation process through which freshwater (permeate) is obtained from seawater under pressure. The subsystem consists primarily of hydraulic components configured to represent the membrane filtration process.

  Subsystem Components and Operation:

  The following hydraulic components form the RO membrane subsystem:

  - **Hydraulic Flow Rate Sensors**: Monitoring the flow rates of permeate and inflow.
  - **Linear Hydraulic Resistance**: Representing the hydraulic resistance of membranes.
  - **Osmotic Pressure Valve (Pressure Relief Valve)**: Creating a pressure barrier simulation of the membrane's osmotic pressure.

  The pressure relief valve simulates osmotic pressure, permitting fluid passage only above a predetermined pressure threshold, and the hydraulic fluid flow (which represents seawater) encounters resistance, simulating the hydraulic properties of the membrane.

Numerical Modelling and Equations:

Linear Hydraulic Resistance:

The pressure drop in the membrane as a function of flow rate is represented by the linear hydraulic resistance, which is given by:

$$\Delta P = R_h Q \tag{2.22}$$

where:

- ΔP: Pressure difference across the membrane (Pa).
- R_h: Hydraulic resistance (Pa$/(\text{m}^3/\text{s})$).
- Q: Volumetric flow rate through the membrane (m^3/s).

Osmotic Pressure (Pressure Relief Valve):

By only opening when the inflow pressure exceeds the osmotic pressure threshold, the osmotic pressure valve replicates the osmotic barrier. It adheres to the linear relationship:

$$A_{\text{osmotic}} = \begin{cases} 0, & P_{\text{inlet}} < P_{\text{osm}} \\ \text{Linear function of } (P_{\text{inlet}} - P_{\text{osm}}), & P_{\text{osm}} \leq P_{\text{inlet}} \leq (P_{\text{osm}} + P_{\text{range}}) \\ A_{\text{max}}, & P_{\text{inlet}} > (P_{\text{osm}} + P_{\text{range}}) \end{cases} \tag{2.23}$$

where:

- A_{osmotic}: Osmotic valve opening area (m^2).
- P_{osm}: Osmotic pressure setting (Pa).
- P_{range}: Valve regulation pressure range (Pa).

The definition of fluid flow across the valve is:

$$Q = C_d A_{\text{osmotic}} \sqrt{\frac{2\Delta P}{\rho}} \tag{2.24}$$

where:

- Q: Flow rate through the osmotic valve (m^3/s).
- C_d: Discharge coefficient.
- ρ: Fluid density (kg/m^3).
- ΔP: Pressure difference across the osmotic valve (Pa).

Subsystem Parameters:

The numerical values of the parameters used in the model are summarized below:

Table 2.8: RO Membrane Parameters[42]

Parameter	Value	Unit
Osmotic pressure	30	bar
Feed salinity (C_m)	$35,946$	ppm
Membrane area (A_m)	35.3	m^2
Number of membranes	183	–

Table 2.9: Linear Hydraulic Resistance Parameters [35]

Parameter	Value	Unit
Resistance (R_h)	0.6023×10^8	Pa/(m^3/s)

Table 2.10: Osmotic Pressure Valve Parameters [35]

Parameter	Value	Unit
Maximum passage area	3×10^{-1}	m^2
Valve pressure setting	30×10^5	Pa
Valve regulation range	5×10^4	Pa
Flow discharge coefficient	0.7	–

- **Direct Coupling**

  A hydraulic pump or cylinder that is powered by the wave energy converter (WEC) directly pressurizes seawater. After the WEC, the accumulator softens the fluctuating pressure before it enters the RO system. By recovering energy from high-pressure brine and transferring it to the incoming feed, the pressure exchanger-intensifier lowers the net energy requirement for RO. The RO Subunit produces brine and permeate by using stabilized high-pressure saltwater.

  Steps for Numerical Modelling (For MATLAB/Simulink):

  – Utilize the hydraulic cylinder's time-varying WEC velocity as input.
  – Using the polytropic relation, update the accumulator state at each step.
  – Utilizing the pressure exchanger, determine the feed pressure and energy recovery.
  – Calculate the RO unit's salt and water flux.
  – For system performance, measure all fluxes (permeate, brine).

2.3. Coupling with Desalination Unit

This section describes how to integrate the reverse osmosis (RO) desalination subsystem and wave energy converter (WEC) systems with the piston in Simulink. The link ensures that the force generated by hydraulic resistance is precisely fed back into the WEC model and that mechanical energy collected from waves is transmitted to the hydraulic desalination unit. This creates a physically realistic, two-way interaction between the energy converter, the desalination process, and the ocean.

2.3.1. Coupling of Heaving Point Absorber WEC Desalination Device

The linear velocity of the floating buoy in the heave direction is the crucial coupling parameter for the heaving point absorber (RM3). The WEC-Sim model produces this velocity, which is then directly linked to the double-acting hydraulic cylinder's input in the piston and RO subsystem. The vertical motion is transformed into a pressurized hydraulic flow by the double-acting hydraulic cylinder, which drives the remaining desalination process.

The hydraulic cylinder's output force, is sent back to the WEC-Sim block as a reaction force. This force is the resistance to the buoy's motion that the hydraulic circuit, including the desalination load imposes. The simulation completes the physical loop by feeding this force back, the buoy experiences an increase in mechanical resistance as the RO unit and hydraulic components require greater force to desalinate water. This two-way coupling ensures that the desalination subsystem and the WEC react to one another dynamically, producing realistic power transfer, load variation, and general efficiency.

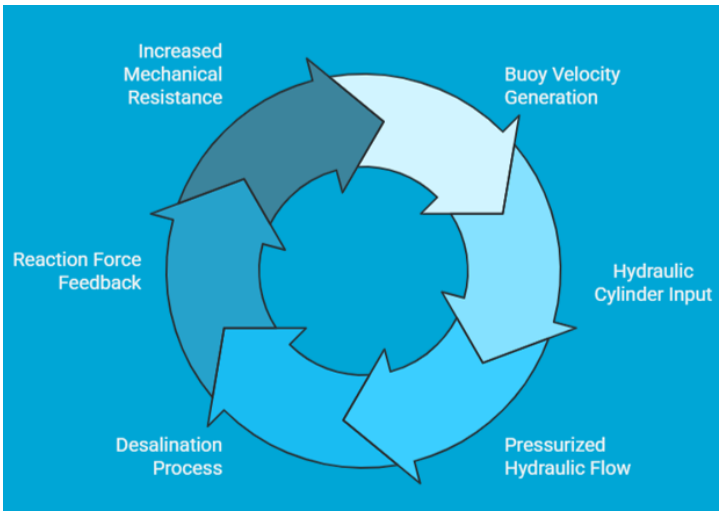

Figure 2.14: Coupling of Heaving WEC and RO unit

2.3.2. Coupling of Oscillating Surge WEC Desalination Device

When using an oscillating surge device (OSWEC), the flap's initial rotational motion is transformed into a linear velocity that is compatible with the hydraulic cylinder input by use of a mechanical linkage or a mathematical block. The hydraulic circuit is driven by this linear velocity, which is once more supplied to the double-acting hydraulic cylinder in the piston and RO subsystem.

The OSWEC system then receives the hydraulic cylinder's output force, which is measured similarly to the heaving device. This force, which reflects the dynamic resistance of the hydraulic and desalination units, acts as a load opposing the flap's rotation. The force sent back to the WEC increases as hydraulic resistance rises (for instance, as a result of the RO membrane's high pressure demands), which slows the flap's motion and affects the energy capture.

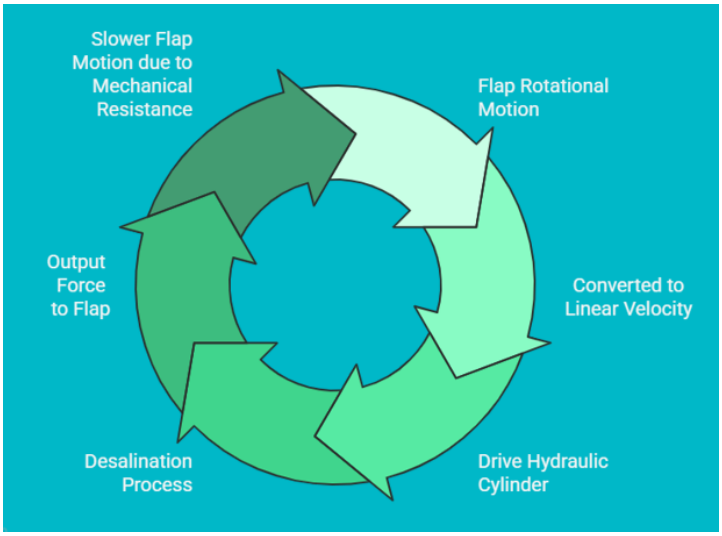

Figure 2.15: Coupling of Oscillating Surge WEC and RO unit

2.4. Simulation Setup

A systematic simulation setup was created in WEC-Sim to examine the performance of the oscillating surge device (OSWEC) and the heaving point absorber (RM3). The primary goal was to ensure steady-state, practical performance measures while assessing the coupled wave energy converter–desalination system in a variety of sea conditions.

Testing Sequence

To verify that the linked model was operating correctly, a baseline test under "no wave" conditions was conducted before the simulation series started. Regular waves with predetermined heights and times were then added. The basic dynamics and the model's convergence to steady-state were confirmed by these experiments. Lastly, using the JONSWAP (JS) spectrum [17] with a peak enhancement factor γ =3.3 for the JONSWAP spectrum, which was first determined in the JONSWAP experiment and is frequently used in the literature for North Sea wave modeling (Hasselmann et al., 1973[17]; Beels et al., 2007[3]; Rusu and Onea, 2021[30]), a thorough set of irregular wave simulations was run. By taking into consideration both peak augmentation and randomness that are common in natural sea states, this spectrum more closely resembles actual ocean waves. The spectrum can be visualized for a particular sea state in Figure 2.16.

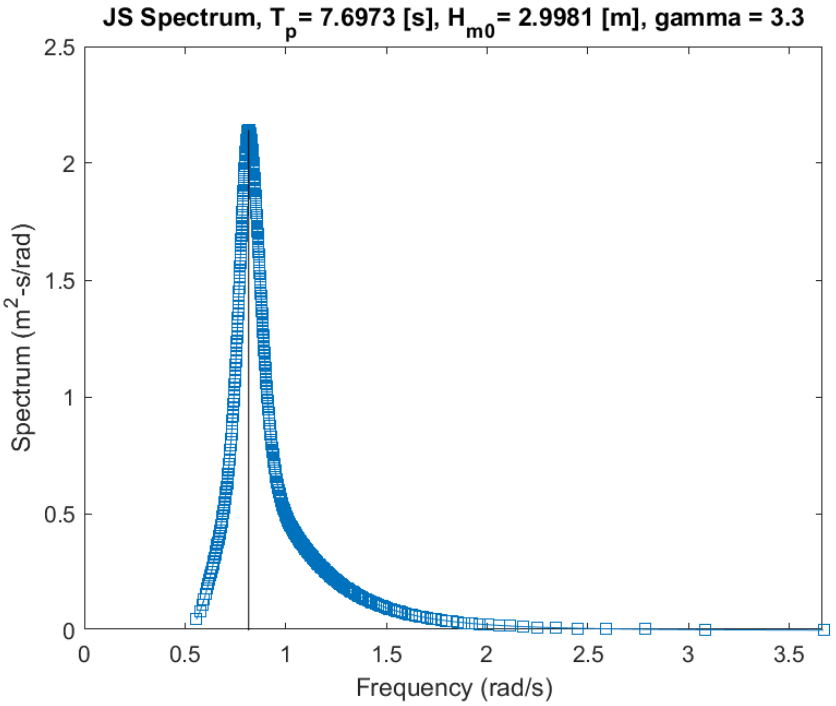

Figure 2.16: JONSWAP spectrum as used for sea state H$_s$= 3m and T$_e$= 7s

Simulation Parameters:

- In order to allow the system to reach steady-state and compute meaningful averages, the simulation time for each example was set at 1000 seconds.
- For the convolution integral, which simulates the fluid memory effects in the radiation force, to be calculated accurately, the simulation time-step has to be 0.01 seconds.
- Wave conditions: Five distinct significant wave heights (1, 2, 3, 4, 5 meters) and five distinct energy periods (5, 6, 7, 8, 9 seconds) were used for the irregular wave testing for both devices, spanning a wide operating window. These parameters guarantee that the performance matrices are thorough by defining a total of 25 distinct sea states. The wave elevation over time can be visualised in Figure 2.17 for the same sea state of H$_s$=3m and T$_e$= 7s.

Radiation Force Modeling

Both input files captured the fluid memory effects that affect device dynamics by including the convolution integral in the radiation force calculation. For accurate time-domain modeling of wave energy devices, this feature is crucial.

Device and Mooring setup:

- Body characteristics, mass, inertia, and Morison elements were adjusted for the OSWEC to correspond with nearshore deployment. The sea depth used in the simulation was 10.9 m.
- The RM3's hydrodynamic characteristics were modified at a water depth of 200 meters, and MoorDyn integration was used to define the mooring system.
- In both situations, the hydraulically driven desalination unit received all available energy, therefore the power take-off (PTO) damping was set to zero.

Steady-State Averaging

Only data from 500 to 1000 seconds (after the initial transient phase) were used for analysis because the models require some time to stabilize. Calculated performance measurements are guaranteed to be accurate and unaffected by start-up impacts because of this steady-state window.

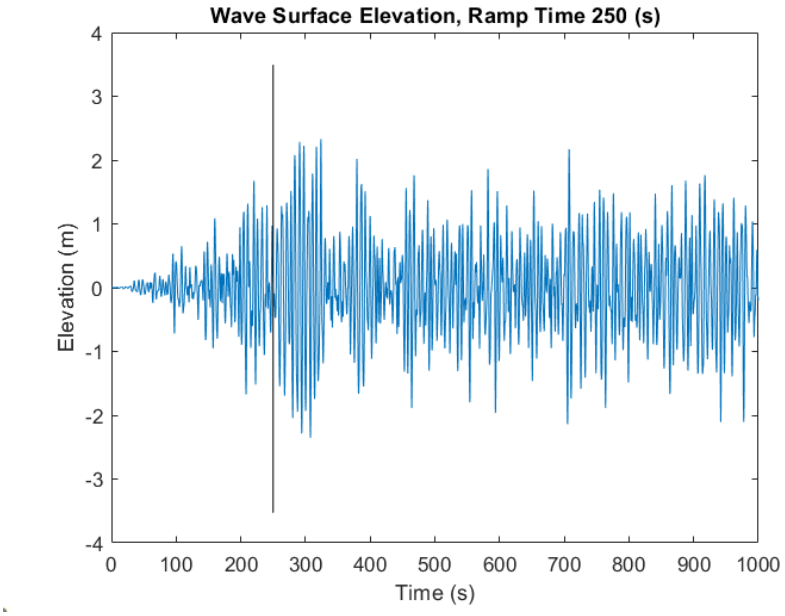

Figure 2.17: Wave Elevation over time as used for sea state H$_s$= 3m and T$_e$= 7s

Automated Post-Processing:

A custom MATLAB script was used to automatically process results from each simulation run. The WEC-Sim Multiple Condition Run (MCR) programming package was used to effectively simulate and examine the response of the system across a variety of sea states. Running multiple simulations with various combinations of significant wave heights and energy periods is automated by the MCR framework. By automatically adjusting the wave parameters in each simulation, MCR systematically ran 25 distinct scenarios for this research, representing each combination in the 5x5 power matrix. This package guarantees consistency and repeatability across all scenarios in addition to saving time and reducing manual involvement. The MCR program gathers and saves the output data from each simulation, which is subsequently utilized for post-processing and the generation of thorough performance matrices. Strong and statistically significant conclusions were supported by the effective mapping of the performance of both WEC devices under various sea states made possible by the workflow's inclusion of MCR.

- Time series data for water permeate flow, force, velocity, and mechanical power are extracted by the script.
- Each parameter's time-averaged values are then determined.
- For each sea state, derived metrics are calculated, including specific water production (m³/kWh), specific energy consumption (kWh/m³), average mechanical power (in kW), average daily water production (in m³/day), and the permeate solute concentration (in ppm).

Visualization

For each simulation, the SimMechanics Explorer (Mechanics Explorer) was turned on to ensure that the devices' physical movements were realistic. Before additional analysis, this visualization tool made sure the model captured real-life dynamics by enabling a close examination of the devices' behavior and interactions with waves.

The findings are then displayed as heat maps, where each output variable is represented by a 5x5 matrix with energy period (Te) on the x-axis and significant wave height (Hs) on the y-axis. This offers a concise visual summary of the device's performance, indicating both ideal and less-than-ideal circumstances for energy consumption and desalination output.

3

Results and Discussions

3.1. Desalination Results

This section initially presents and thoroughly explains the results of a single typical simulation in the results sections for the OSWEC oscillating surge device and the RM3 heaving point absorber. The sea condition with a significant wave height (Hs) of 3 meters and an energy period (Te) of 7 seconds is the subject of the analysis. By choosing this instance, the report describes how each device functions in the time domain, capturing the rotating or heave motion during a 1000-second simulation period. In both devices, the reverse osmosis desalination unit is driven by the mechanical motion of the sea, which is directly transferred into the hydraulic system. This approach makes it easier for the reader to follow along as the wave energy is converted into hydraulic power, which desalinates saltwater while the RO membrane creates freshwater. As the system enters steady-state operation, the results in these comprehensive sections display key outputs such as the float or flap's displacement and velocity, the mechanical power sent to the desalination unit, and the rate of freshwater (permeate) production.

The section first presents the findings for this particular sea state before going over the full set of simulations carried out using the Multiple Condition Run (MCR) which helps automate the process of simulating all 25 sea states considered by simulating each combination of sea state and storing the results in arrays and using all of the stored data for post-processing. The simulations provide a general investigation of system performance by incorporating all 25 possible combinations of five energy periods and five significant wave heights. The section aggregates steady-state outcomes for each scenario during the last 500 simulation seconds as this window ensures only steady-state dynamics are captured by the system, and a similar approach has been implemented by (Yu and Jenne, 2018[42]). The ramp-up time for all simulations is defined as 250 seconds, which ensures the system accommodates all the transient effects gradually and then enters steady state. Heatmaps and matrices summarizing these averaged results for important parameters are included in the Power Matrices for Both Devices and Comparative Analysis section. This makes it possible to directly and clearly compare the effectiveness and performance of both kinds of wave energy converters in a broad range of sea conditions for the studied water depths.

3.1.1. Heaving Point Absorber WEC Desalination Results (H_s= 3m, T_e= 7s)

The RM3 heaving point absorber was simulated for 1000 seconds in the selected sea condition with a significant wave height of 3 meters and an energy period of 7 seconds. The average values for all important parameters were computed using only the steady-state performance, which was extracted from the 500–1000 second range and can be visualized in Figure 3.1.

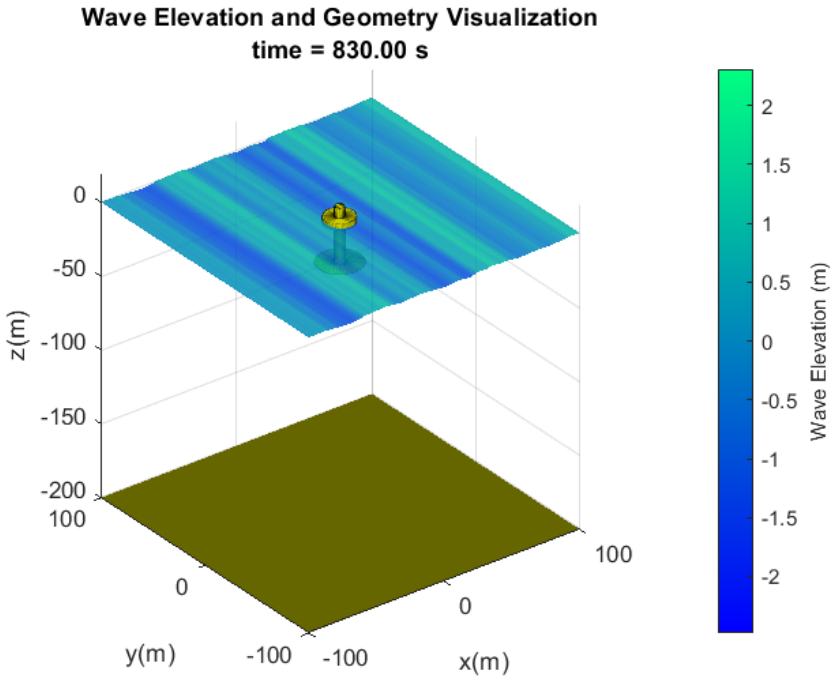

Figure 3.1: Heaving RM3 WEC visualization as used for sea state H$_s$= 3m and T$_e$= 7s

The location, velocity, and acceleration data showed strong, irregular changes, and the float (Body 1) showed noticeable vertical oscillations. The device successfully gathered wave energy from moderate sea conditions, as illustrated by the amplitude of the float's heave reaching values exceeding one meter during the simulation. As the reaction mass, the spar (Body 2) additionally showed noticeable but less prominent oscillations, offering a steady surface for energy absorption and transfer and is clear in Figure 3.2.

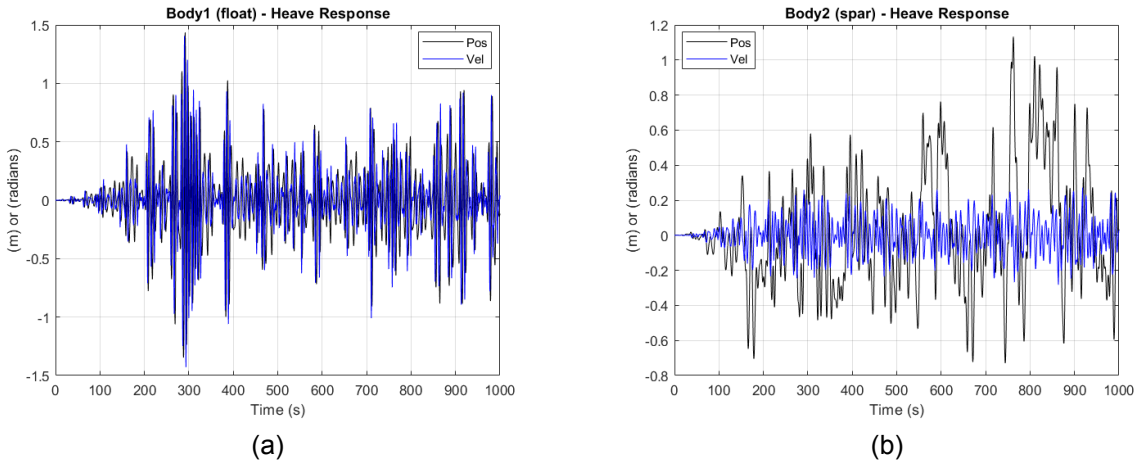

Figure 3.2: Heave Response over time on RM3 Device components: (a) Float (b) Spar

Excitation, radiation damping, added mass, restoring components all contributed to the hydrodynamic forces acting on the float. Together, these forces created a total force that fluctuated in strength and direction, closely resembling the float's up-and-down movement and the incident wave characteristics as seen in Figure 3.3. In order to ensure accurate numbers for a practical performance evaluation, the time-averaged mechanical power transferred as seen in Figure 3.4 from the RM3 to the hydraulic and desalination subsystem was computed for the steady-state interval.

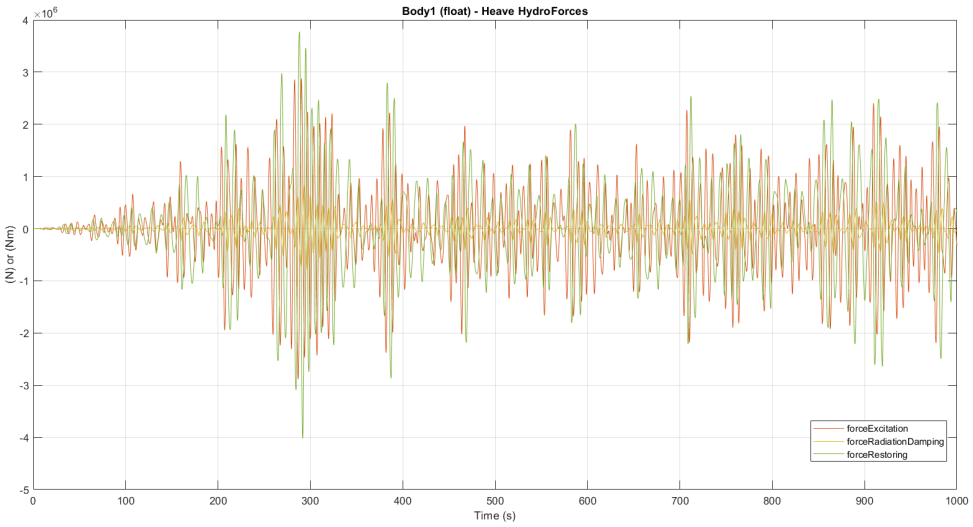

(a)

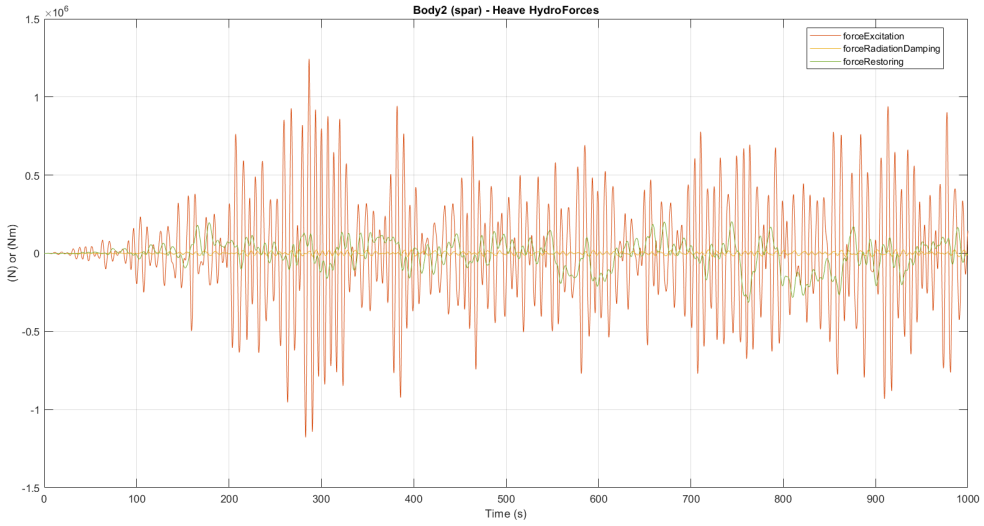

(b)

Figure 3.3: Heave Forces over time on RM3 Device components: (a) Float (b) Spar

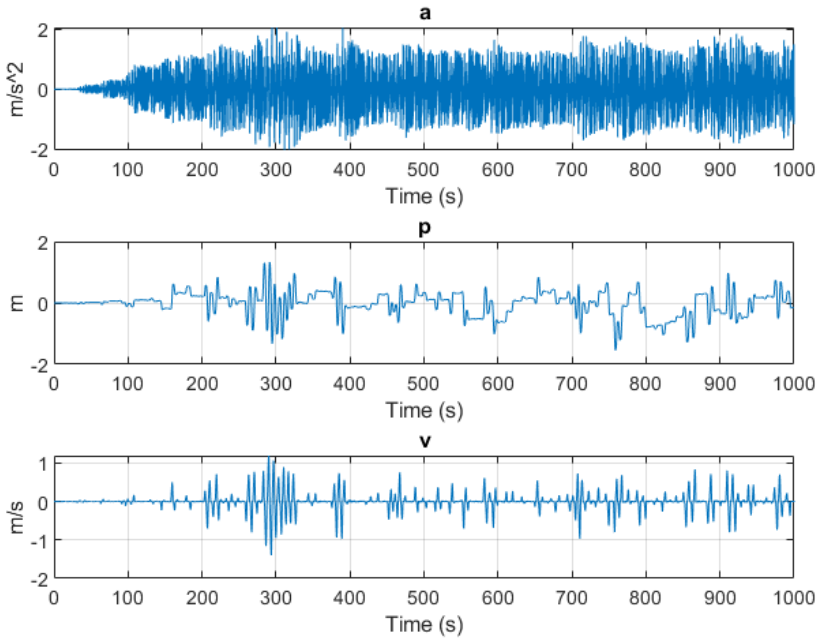

Figure 3.4: Acceleration, Position, and Velocity over time as captured by the PTO for RM3 Heaving Device

As the hydraulic pressure accumulated, the desalination subsystem's permeate flow rate (freshwater production) first increased before rapidly stabilizing during the steady-state phase. The overall rate of water production stayed non-zero over time after the osmotic pressure build-up, suggesting that wave energy was reliably converted into freshwater. The average power supplied to the RO unit and the average daily water output were used to compute the simulated specific energy consumption (SEC) and specific water production (SWP).

Both the freshwater production rate and the osmotic pressure across the reverse osmosis (RO) membrane were monitored over time while simulating the RM3 heaving point absorber for a sea state with a significant wave height of 3 meters and an energy period of 7 seconds.

The RM3 device successfully converted wave energy into hydraulic pressure appropriate for reverse osmosis desalination during the time-domain simulation for this moderate-to-high energy sea state. During the first 150–200 seconds of the simulation, the osmotic pressure across the RO membrane increased gradually until it reached the desired value of roughly $3{\times}10^6$ Pa as seen in Figure 3.5. Following this quick increase, the system kept the pressure high for the duration of the run. Because it ensures that the RO process runs smoothly and that the membrane has sufficient driving force to separate freshwater from saltwater, this steady pressure is crucial.

The water production rate (permeate flow, Q) exhibited a similar time-dependent pattern. Initially, as system pressure increased, water production increased as well. The water production rate indicated clear peaks and troughs when the osmotic pressure reached its fixed value, changing in response to the pressure and mechanical input fluctuations. Over the course of the simulation's steady-state phase, the average permeate flow remained consistently non-zero in spite of these natural oscillations that are common for wave-driven systems and can be visualized in Figure 3.6.

These results indicate that the RM3-driven desalination system can continuously produce freshwater while rapidly creating and sustaining the required operating pressure for RO under the selected sea state. As the system ramps up, the initial transient behavior is normal, however, once steady state is reached, both pressure and water production are consistent. This confirms that the RM3 can offer consistent, dependable desalination in offshore locations with comparable wave conditions.

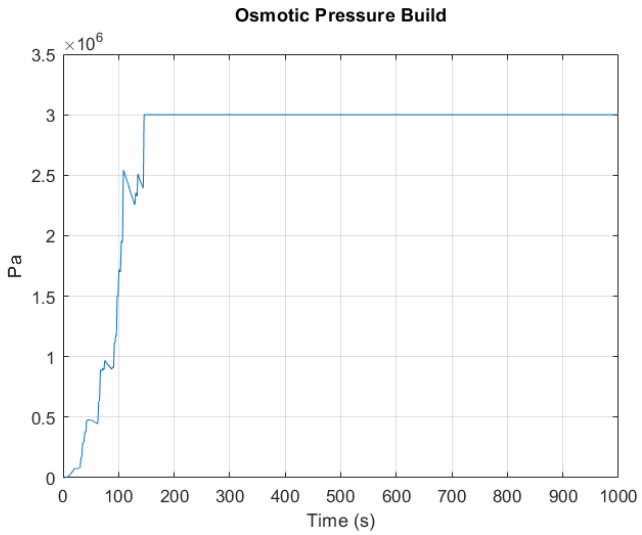

Figure 3.5: RM3 Osmotic Pressure Build for sea state H$_s$= 3m and T$_e$= 7s

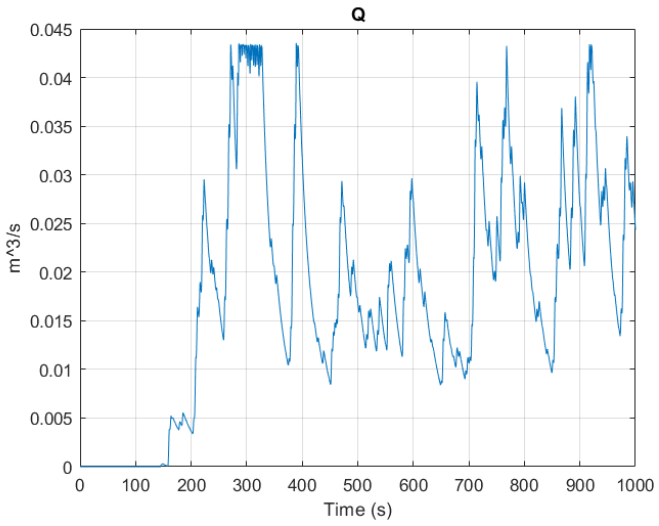

Figure 3.6: RM3 Water Production for sea state H$_s$= 3m and T$_e$= 7s

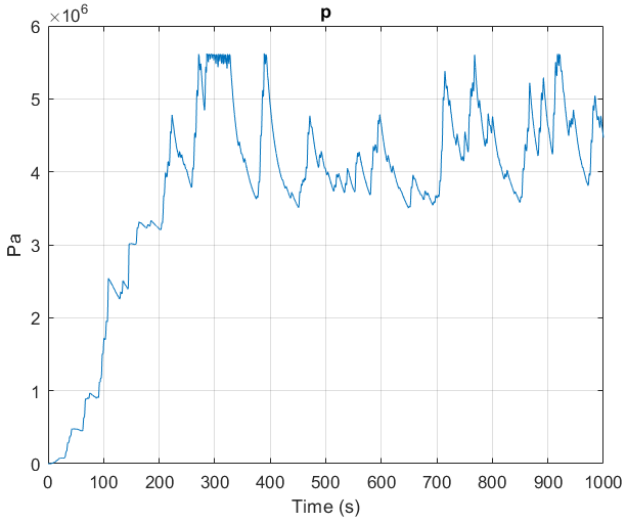

Figure 3.7: RM3 Pressure variation over time before RO membarane for H$_s$= 3m and T$_e$= 7s

At Hs = 3 m and Te = 7 s, the pressure variation for the RM3 device prior to the RO membrane as seen in Figure 3.7 has a typical transient rise followed by fluctuations around a relatively constant value. When the system first starts up, the pressure rises quickly before plateauing at roughly 5 MPa after 200 seconds. Smaller oscillations that represent the dynamics of the hydraulic system and the variability of wave-driven input are scattered across this plateau. Although the system as a whole is able to maintain a high pressure appropriate for RO desalination, these oscillations are to be expected because the irregular wave input affects the pressure.

3.1.2. Oscillating Surge WEC Desalination Results (H_s= 3m, T_e= 7s)

The OSWEC was simulated across a 1000-second time domain for the sea condition characterized by a significant wave height of 3 meters and an energy period of 7 seconds and can be visualized in Figure 3.8. With considerable surge motion, the OSWEC's flap reacted dynamically to the incoming waves. The flap's position, acceleration, and velocity all displayed oscillatory patterns during the simulation, with distinct peaks and troughs that corresponded to the wave input's variability. As expected, the moving flap captured and transformed the wave energy into rotational and translational motion, while the stationary base remained fixed which is observed in Figure 3.9.

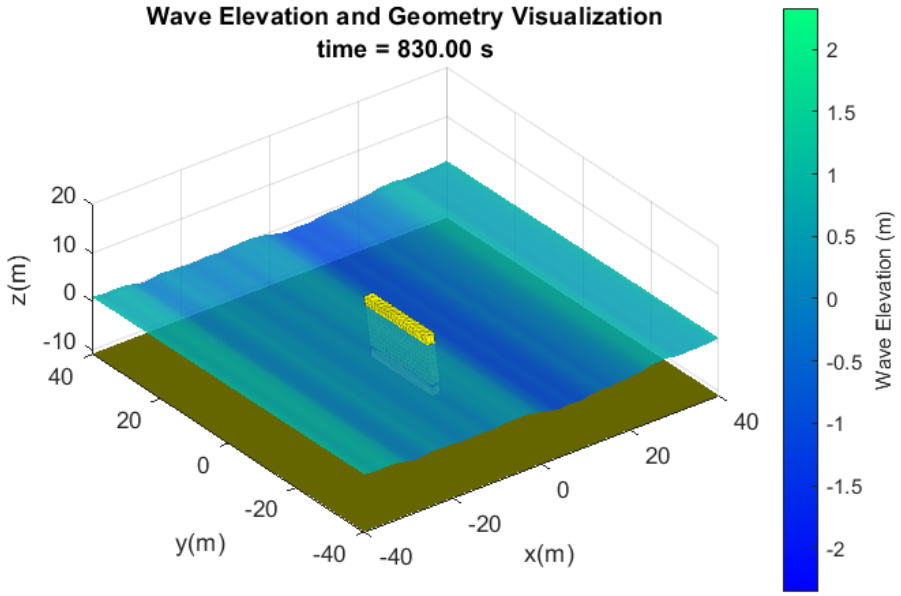

Figure 3.8: Oscillating Surge WEC visualization as used for sea state H$_s$= 3m and T$_e$= 7s

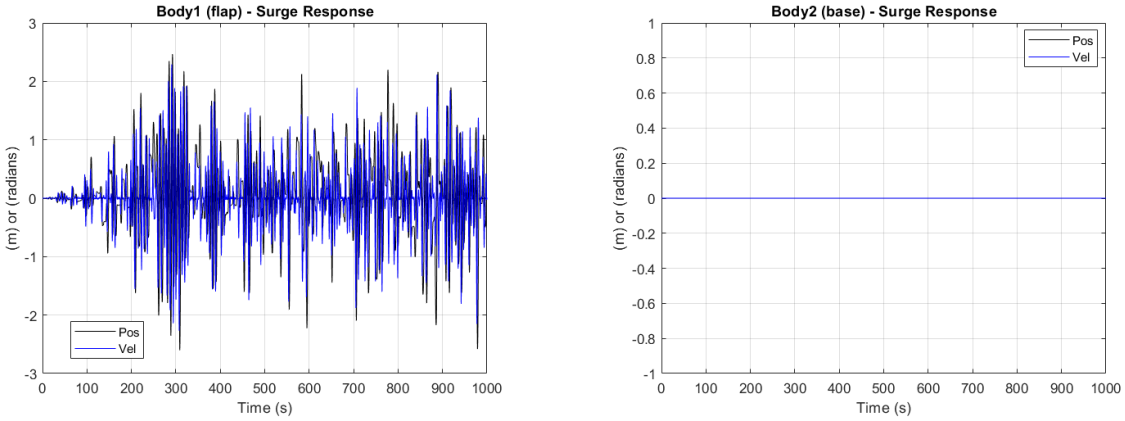

(a) (b)

Figure 3.9: Surge Response over time on OSWEC Device Components: (a) Flap (b) Base

The OSWEC's hinged flap actively responded to the incident waves during the simulation, experiencing massive surge motions with irregular oscillating behavior. As the wave force increased, the flap's position, velocity, and acceleration all increased in magnitude. This was indicative of the unstable

nature of the wave input, as it reached a regime where high-frequency oscillations persisted. As a solid reaction point for the moving flap, the device's base, attached to the seabed, remained fixed which is clearly shown in Figure 3.10.

The overall force needed to drive the device was influenced by a variety of hydrodynamic forces acting on the flap, including excitation, radiation damping, added mass, restoring, viscous, and linear damping. These forces changed dynamically throughout time. As the flap moved, the total force and its individual components fluctuated, reaching maximum and minimum values that corresponded to the surge's peaks and troughs.

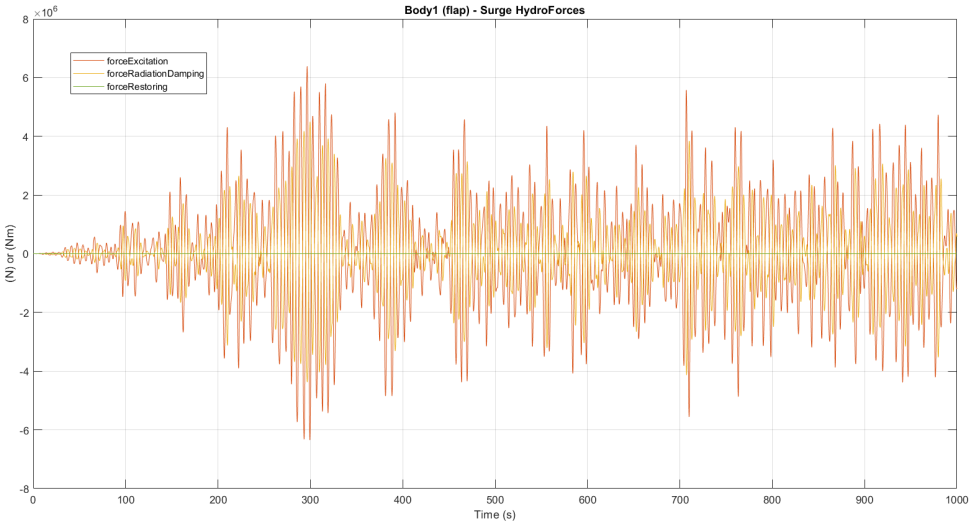

(a)

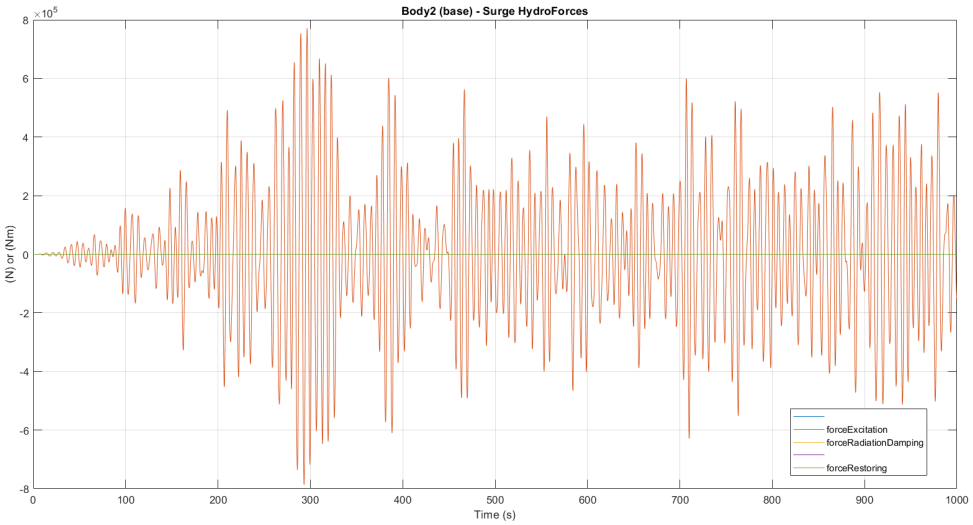

(b)

Figure 3.10: Surge Forces over time on OSWEC Device Components: (a) Flap (b) Base

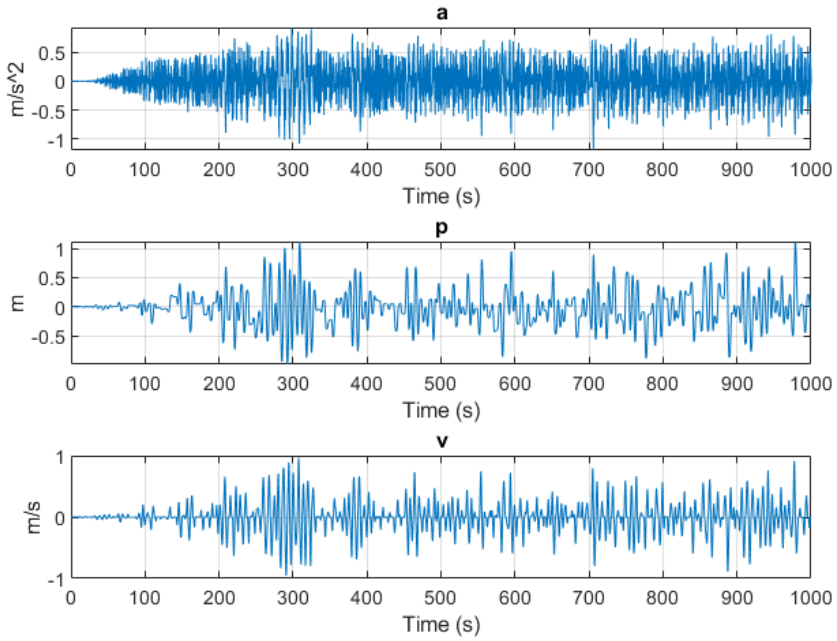

Figure 3.11: Acceleration, Position, and Velocity over time as captured by the PTO for OSWEC Oscillating Surge Device

The oscillating surge wave energy converter (OSWEC) effectively converted mechanical wave energy into hydraulic pressure as seen in Figure 3.11for the reverse osmosis (RO) desalination subsystem during the simulation for this moderate sea state. In the first 100 seconds of operation, the osmotic pressure across the RO membrane increased significantly, reaching and then sustaining steady at about 3×10^6 Pa for the duration of the simulation. Since a significant pressure differential across the membrane is required to push water molecules from the saline to the fresh side, this rapid build-up and steady maintenance of high pressure are essential for efficient desalination which is observed in Figure 3.12.

There was a similar time-dependent trend in the water production rate (permeate flow). Initially, as system pressure increased, the flow rate increased steadily. The water production rate peaked once the osmotic pressure stabilized, primarily ranging from 0.025 to 0.045 m^3/s in steady-state operation as observed in Figure 3.13. In wave-driven systems, where energy input fluctuates according to the sea state and device response, these variations are normal. Throughout most of the simulation time, the overall permeate flow shows that the OSWEC can reliably transform wave energy into a usable freshwater output.

The findings demonstrate that the OSWEC-driven system maintains a non-zero and significant rate of freshwater production while also establishing the high pressure required for reverse osmosis under sea states of 3 m and 7 s. The OSWEC device's ability to handle continuous desalination in realistic, time-varying ocean conditions is demonstrated by its consistent water production and stable pressure.

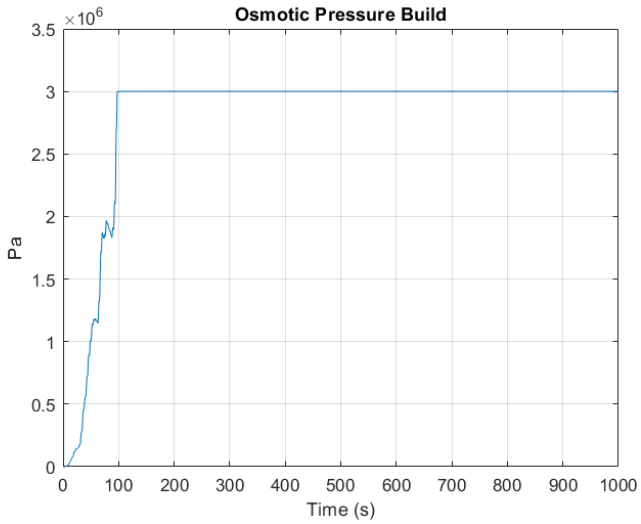

Figure 3.12: OSWEC Osmotic Pressure Build for sea state H$_s$= 3m and T$_e$= 7s

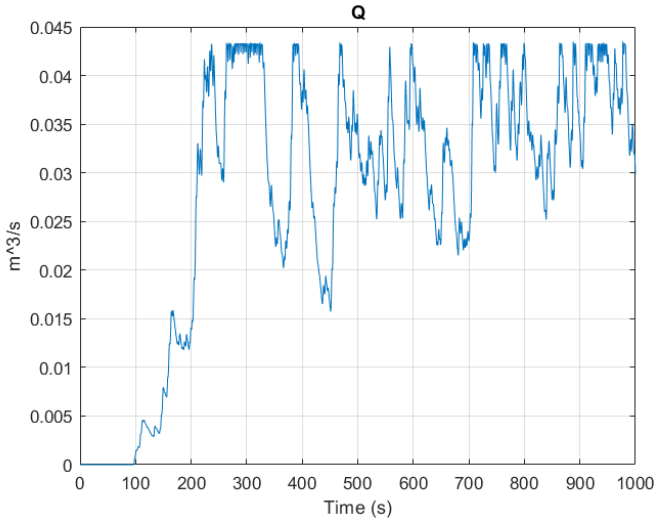

Figure 3.13: OSWEC Water Production for sea state H$_s$= 3m and T$_e$= 7s

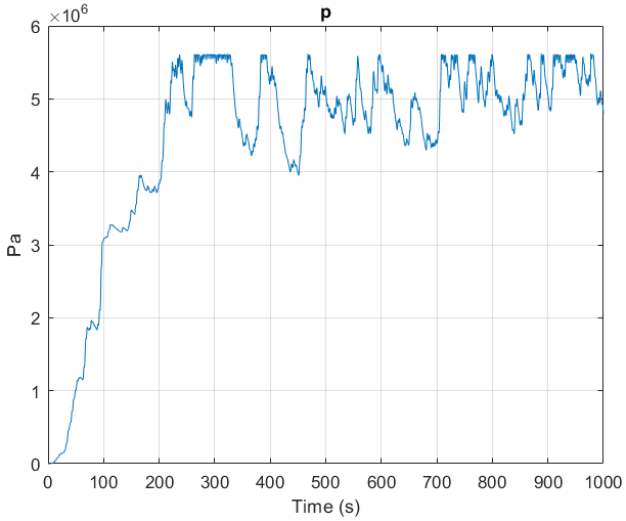

Figure 3.14: OSWEC Pressure variation over time before RO membarane for H$_s$= 3m and T$_e$= 7s

The pressure before the RO membrane of the OSWEC device similarly increases quickly during the initial phase as seen in Figure 3.14, stabilizing at about 5 MPa after 200 seconds. Due to the continuous influence of the wave energy input, the resulting pressure profile stays consistent with slight fluctuations. This consistently high pressure is essential for RO operation and shows that, despite of the wave environment's variability, the OSWEC device continuously maintains the conditions required for desalination. Good system control and efficient hydraulic energy transmission from the OSWEC to the RO chamber is shown by the pressure consistency over the osmotic pressure.

3.1.3. Matrices for Both Devices

A matrix of the results was created from 25 distinct sea state combinations in order to thoroughly evaluate the performance of the OSWEC oscillating surge device and the RM3 heaving point absorber. Significant wave heights between 1 and 5 meters and energy periods between 5 and 9 seconds characterize each sea state. The Multiple Condition Run (MCR) program, which effectively performs each combination and handles the resulting data, has been employed to conduct the simulations for each of these cases.

Time-domain results for the steady-state window of 500–1000 seconds were extracted for every simulation. Absolute velocity, force, mechanical power, and permeate flow rate from the RO unit are among the important mechanical and desalination parameters whose average values are determined by the code. After converting the permeate flow to the average daily water output (m³/day), the post-processing script computes two crucial performance metrics: Specific Water Production (SWP) in m³/kWh and Specific Energy Consumption (SEC) in kWh/m³. SWP shows how much freshwater is produced for every unit of energy used, whereas SEC is the ratio of total energy intake to water produced.

The RM3 device's results are displayed in Figures 3.15, 3.17 and 3.19. The matrix shows very high values for SEC at low wave heights, particularly for short durations, which suggests low efficiency in these conditions. SEC sharply decreases with increasing wave height, stabilizing below 5 kWh/m³ in the majority of higher sea conditions. RM3 produces very little water on average for low Hs, but when wave height and period grow, production increases rapidly, reaching around 3000 m³/day in the most dynamic sea conditions. The desalinated water only reaches acceptable drinking water quality at the highest wave heights and times, according to the permeate concentration heatmap for the RM3 device. Concentrations are much higher in lower sea states, often exceeding 1000 parts per million. This demonstrates the device's inability to produce high-quality water outside of optimum sea conditions, suggesting the need for further pretreatment or optimization steps.

The OSWEC results are shown in Figures 3.16, 3.18 and 3.20. The OSWEC, which mostly ranges between 2 and 4.5 kWh/m³, has more constant SEC values throughout various sea states than RM3. The highest wave states exhibit higher SEC values, most likely as a result of less ideal energy transmission and higher device loading. Even at low wave heights, the OSWEC generates significant amounts of water, and output increases gradually for greater Hs and Te. When sea conditions are low to moderate, the maximum daily water production exceeds 3500 m³/day, exceeding RM3. In all tested sea states, the OSWEC results are noticeably better. For most medium to high sea conditions, the permeate concentration stays below 600 ppm, suggesting that the system is effective in meeting WHO criteria for drinkable water. Concentrations surpass 1000 ppm only at the lowest wave height, confirming OSWEC's capability for dependable desalination even under mild conditions.

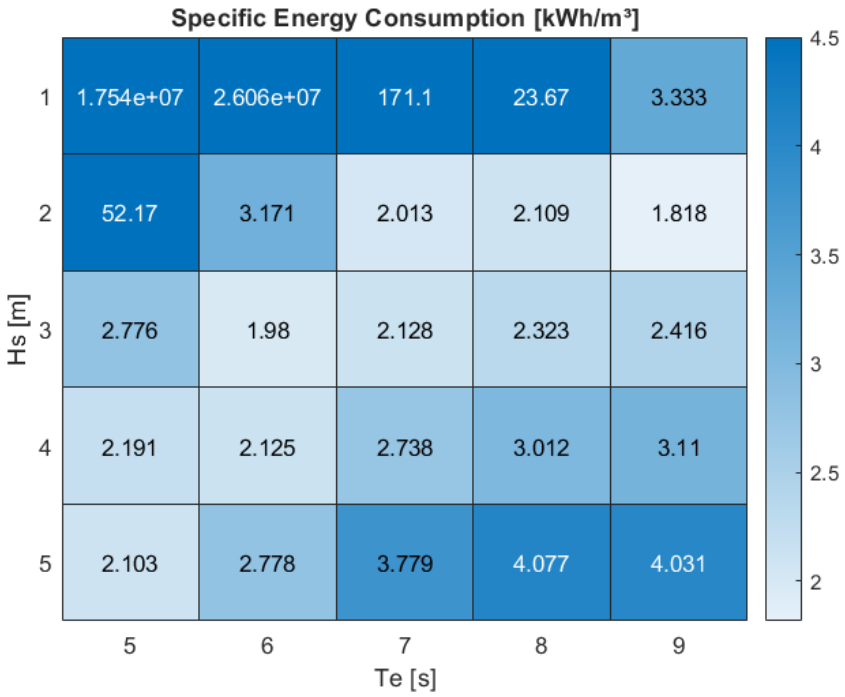

Figure 3.15: SEC Power Matrix for Heaving RM3 Device with Mooring

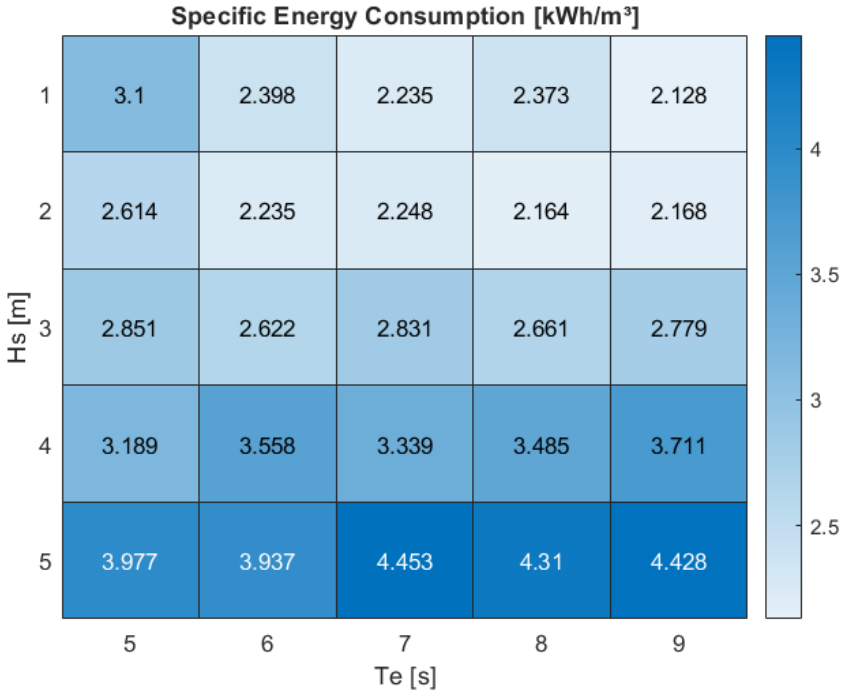

Figure 3.16: SEC Power Matrix for Oscillating Surge WEC

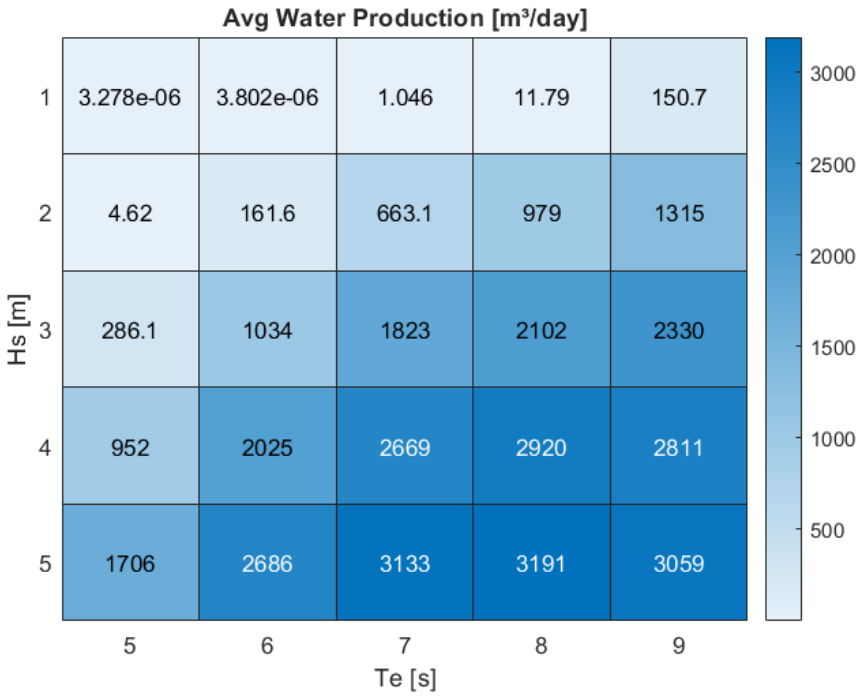

Figure 3.17: Average Water Production per day Matrix for Heaving RM3 Device with Mooring

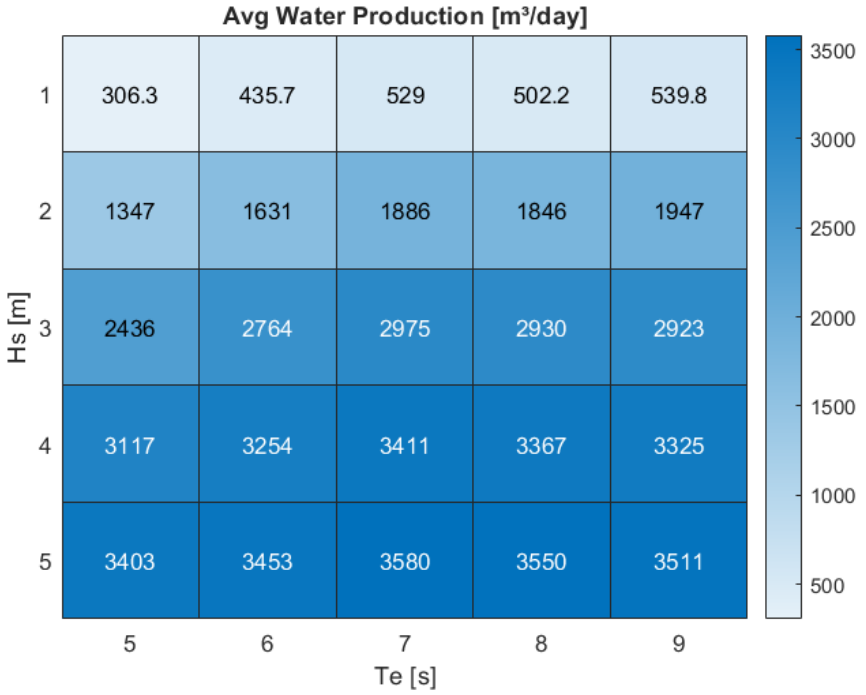

Figure 3.18: Average Water Production per day Matrix for Oscillating Surge WEC

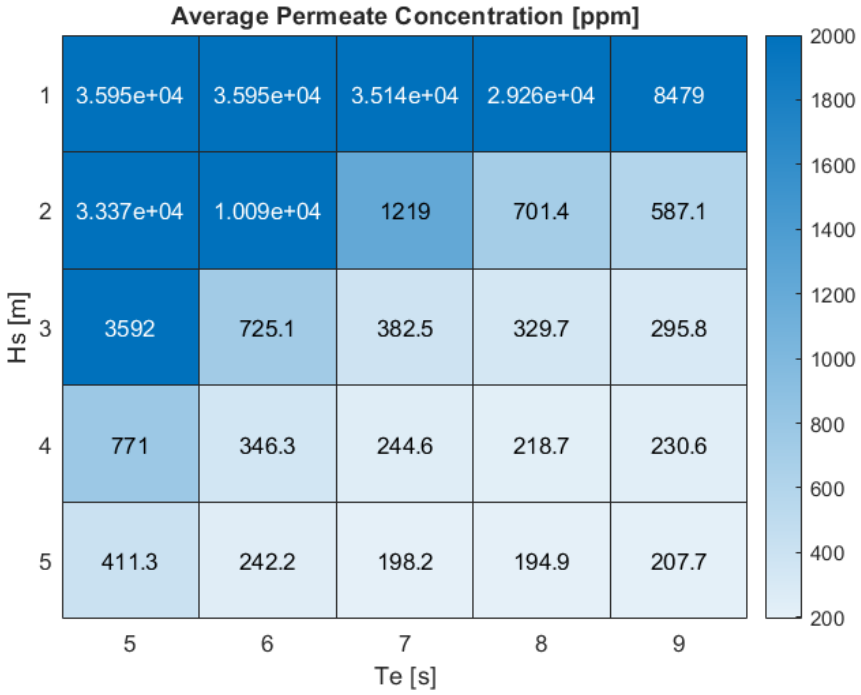

Figure 3.19: Average Permeate Concentration Matrix for Heaving RM3 Device with Mooring

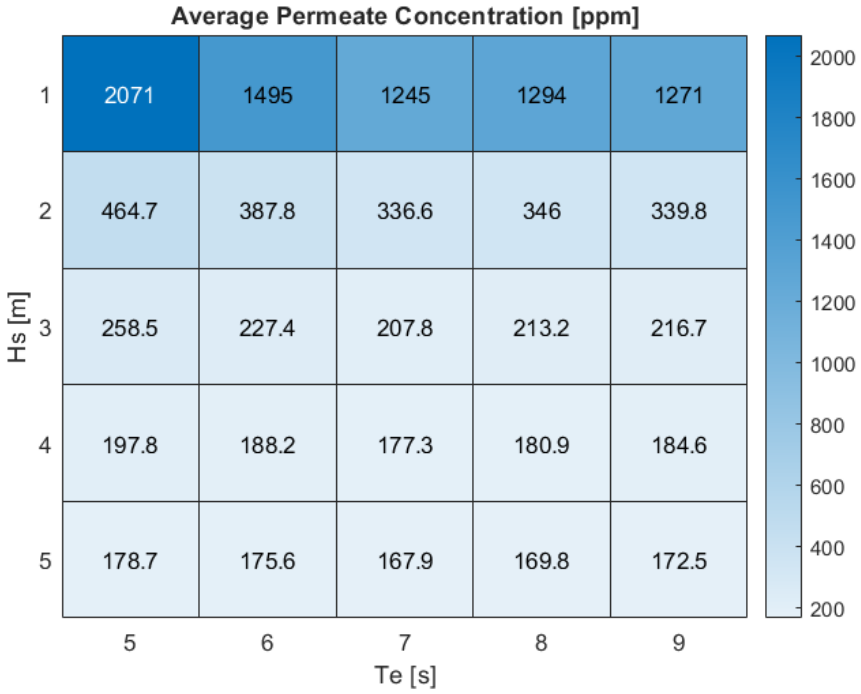

Figure 3.20: Average Permeate Concentration Matrix for Oscillating Surge WEC

The performance of the devices in actual ocean conditions can be clearly and quantitatively compared because of these matrices. It is simple to determine the most suitable sea conditions for energy-efficient desalination according to the heatmap visualization, which also shows how each device reacts to shifting wave regimes. Results for both WEC-desalination configurations are ensured to be dependable, averaged across steady-state conditions, and directly comparable because of this approach.

3.1.4. Comparative Analysis

The performance of the OSWEC oscillating surge device and the RM3 heaving point absorber as wave-driven desalination systems throughout 25 sea state combinations is the main subject of this section's comparison. The main factors taken into account in the analysis are average daily water output, average permeate concentration, and specific energy consumption (SEC).

The performance of the RM3 device varies greatly depending on the sea condition. The SEC values for RM3 are extremely high for low wave heights and short energy periods, they are frequently many orders of magnitude higher than realistic desalination goals. This suggests that when there is little wave energy available or when the waves are short and steep, the RM3 is inefficient. However, the SEC values decrease significantly, occasionally falling below 3 kWh/m³, when the energy period lengthens and the major wave height rises, particularly over 3 meters. Alongside this comes a sharp increase in water production, which in the highest sea states can exceed 3000 m³ per day. In dynamic situations, the RM3 performs much better, but in calm or moderate seas, its efficiency gradually declines.

On the other hand, the OSWEC performs more consistently throughout the whole sea state matrix. In the most severe wave circumstances, its SEC values only gradually increase, typically staying between 2 and 4.5 kWh/m³. With a steady increase in daily water output as sea states grow more energetic, the OSWEC, in contrast to the RM3, maintains moderate water production even at lower wave heights. The maximum output exceeds 3500 m³ per day, and the device exhibits significantly reduced responsiveness to low-energy circumstances. In a wide range of sea situations, the OSWEC performs better than the RM3 at generating permeate with reduced salinity. In lower sea conditions, the OSWEC achieves better desalination performance and dependability, but RM3 finds it difficult to reach drinkable limits. This consistent supply implies that the OSWEC is more adaptable and capable of delivering freshwater consistently throughout a larger variety of ocean climates.

The RM3 is significantly less effective in mild or moderate seas, even though it can outperform the OSWEC in the states with the highest wave energy. However, the OSWEC is the most reliable and practical option for desalination in a variety of sea conditions throughout the year since it offers more regular water output and energy efficiency.

3.1.5. Interpolation of Results for Desired Sea States

Power matrices for the OSWEC oscillating surge device and the RM3 heave device were developed in the earlier sections. For specified values of significant wave height and wave energy period, these matrices provide performance measures including specific energy consumption (SEC) and average water output. It might be essential to estimate these values for additional sea states that were not directly simulated, even though the simulations were run at discrete points. Interpolation techniques are utilized to do this, which makes estimating values within the known data range simple.

This method uses bilinear interpolation to estimate values between known data points, ensuring accurate and consistent predictions. A 5x5 matrix of SEC and water production values was generated for each device, which corresponded to wave heights ranging from 1 to 5 meters and periods ranging from 5 to 9 seconds. The primary dataset for interpolation is made up of these matrices.

Two desired values of Te and Hs are chosen in order to estimate values at intermediate sea states. Together with the established matrices for SEC and water production, the MATLAB code specifies the original vectors for Hs and Te. For each sea condition that falls within the initial simulation range, this procedure can be easily repeated.

For example, the interpolation provides the corresponding SEC and average daily water production values when a sea state with Hs = 3.5 m and Te = 7.5 s is taken into consideration and the results are presented in Table 3.1. It is crucial to remember that interpolation only produces correct findings within the initial range of sea states that were evaluated. Because of the possibility of errors, extrapolation or estimating beyond tested values, should be done with caution.

More thorough evaluations of these wave energy-driven desalination systems are made possible by the interpolation process, which enables engineers and designers to rapidly predict device performance for a variety of ocean conditions.

Table 3.1: Interpolated results for RM3 and OSWEC devices

Device	H_s (m)	T_e (s)	SEC (kWh/m^3)	Water Production (m^3/day)
RM3	3.50	7.50	2.550	2378.50
OSWEC	3.50	7.50	3.079	3170.75

According to (Beels et al., 2007[3]), the characteristic distribution of North Sea wave climates is well suited to the interpolation and extrapolation methods used in this research. The sea state matrix includes the empirically observed conditions at important sites like the Belgian shelf (Hs=1.2 m, Te=5.1 s), Ekofisk (Hs=2.2 m, Te=6.3 s), and Haltenbanken (Hs=2.7 m, Te=7.5 s). It was built for significant wave heights between 1 and 5 meters and energy periods of 5 to 9 seconds. The methodology can anticipate WEC-desalination system performance for the great majority of operational conditions that are likely to occur in the region by calibrating the interpolation procedures within this framework. The method's robustness is reinforced by its emphasis on distinctive and frequently recurring sea states, which also guarantees that its findings and suggestions are generally applicable for deployments in the North Sea and other locations with comparable moderate wave energy climates (Beels et al., 2007[3]).

3.2. Discussions

3.2.1. Interpretation of Results

When employed for wave-driven desalination, the results clearly demonstrate the performance differences between the OSWEC oscillating surge device and the RM3 heaving point absorber. Only in energetic sea states with high wave heights and extended energy periods can the RM3 device show good performance. Under these ideal circumstances, its average water production can surpass 3000 m^3/day and its specific energy consumption (SEC) can go below 3 kWh/m^3. However, as seen by its extraordinarily high SEC and essentially nonexistent freshwater production, the RM3 is ineffective in less energetic or more normal coastal sea situations. In contrast, the OSWEC keeps its performance level more constant. It provides moderate to high water production even when waves are weaker, and its SEC stays within a realistic range of 2 to 4.5 kWh/m^3 in almost all studied sea states. Because of its stability, the OSWEC can operate effectively in a wider range of environments and is less susceptible to variations in wave climate. The dynamic coupling between the WEC and desalination subsystems enables fluctuations in power transmission and freshwater production, simulating the sea's variability. Both devices can achieve steady operation in the time domain. The distinct patterns seen in the water production and power matrices provide crucial information about each device's suitability for various real-world deployment scenarios.

The findings show that wave energy may be efficiently converted into freshwater by both RM3 and OSWEC devices. These device's average water output and specific energy consumption (SEC) figures are in close alignment with those of comparable current technology. Similar to or slightly better than the typical wave-powered desalination results of roughly 2.2 to 4.5 kWh/m^3 reported for surge-type devices in the literature as the SEC reduces significantly after the usage of a pressure exchanger, which is evident from the simulations, the OSWEC showed more stable and consistent freshwater production across a range of sea conditions, maintaining SEC primarily between 2 and 4.5 kWh/m^3 (Chakravarthi et al., 2024[4]). The RM3 device, on the other hand, only functioned well in more intense wave conditions and revealed higher variability. Its ideal SEC of 2–3 kWh/m^3 is consistent with point absorber devices of comparable characteristics that have been documented in studies such as Delbuoy (Hicks et al.,1989[18]) and CETO freshwater (Leijon and Bostrom, 2017[22]). These results demonstrate that wave-powered desalination is feasible, but they also highlight how device-specific features have a major impact on overall effectiveness and freshwater yield. These findings show that, in comparison to the RM3, the OSWEC device is more efficient at providing drinkable water quality over a larger range of sea conditions. Higher stability and practical applicability are suggested by the continuously reduced ppm values for OSWEC, especially in coastal regions with moderate wave energy. Also, the RM3 has limitations for wider deployment, even though it might still be useful in areas with higher wave heights.

3.2.2. Limitations and Assumptions

This project's numerical modeling approach is subject to a number of assumptions and limitations that could affect the results. Firstly, the simulations use hydrodynamic coefficients that have already been derived using frequency-domain solvers such as WAMIT. These values assume idealized device geometries and regular wave interaction, which may cause them to ignore certain irregular or three-dimensional flow phenomena. The linearized time-domain hydrodynamic method is the basis of this thesis. In the main WEC and system dynamics, nonlinear forces like higher-order wave excitation or quadratic drag are not taken into account. The models may not account for the effects of local seabed conditions and changing bathymetry in actual deployment sites because they utilize a set water depth (200 m for RM3 and 10.9 m for OSWEC). Although the MoorDyn software incorporates mooring effects, the accuracy of the simulated motions may still be impacted by simplifications in the seabed interaction and mooring line dynamics. In contrast to practical hybrid systems, the power take-off (PTO) system is idealized by assuming that all mechanical energy is used for desalination and modeling it without electrical conversion losses which would have been the case if the PTO was modeled with a non-zero damping coefficient. The reverse osmosis subsystem does not take into consideration potential fouling, membrane degradation, or long-term temperature impacts because it employs standard membrane specifications and assumes a constant salt concentration. Additionally, the simulation's emphasis on average steady-state performance at 500-second intervals might hide crucial events or system start-up/shutdown behavior. Lastly, the JONSWAP [17] spectrum is used to represent the wave climate with a defined set of heights and periods, which may not fully capture the variability observed in nature. When understanding the data's practical consequences, these aspects should be taken into account. Due to these limitations, the results could not accurately reflect performance in the actual world, particularly in extreme, nonlinear, or site-specific conditions. While assumptions on ideal PTO and constant salinity could overestimate efficiency and water quality, the steady-state focus and simplified models may underestimate variability and operational challenges. Therefore, before making decisions about real-world deployment, conclusions should be carefully analyzed and validated against experiments or site-specific studies.

This project's interpolation approach has a number of limitations and presumptions as well. Complex, nonlinear fluctuations that occur in real ocean conditions may not be properly reflected by interpolation, which presumes a linear relationship between the simulated data points. Additionally, predicting parameters close to or just beyond the original data ranges reduces the accuracy of interpolation. Since the approach ignores extreme or unpredictable system characteristics, extrapolation outside of tested sea states adds even more uncertainty and runs the danger of serious errors. In order to ensure reliability, interpolated results should always be interpreted cautiously, particularly when they are close to boundaries, and ideally backed up by more simulations or experimental validation.

Numerous limitations and presumptions are introduced by the interpolation methodology used. Potential nonlinear behavior present in wave-driven systems is ignored by the power matrices for SEC and water production, which assume a linear fluctuation across the tested sea states (Leijon and Bostrom, 2017[22]). Furthermore, especially during extrapolation, the accuracy of the interpolated findings drastically decreases close to the matrices' edges. Predictions that go beyond the first tested wave heights (1–5 m) and times (5–9 s) are therefore loaded with significant uncertainty. Additionally, the method ignores possible operational problems such as membrane fouling, device fatigue, or environmental influences impacting long-term efficiency because it assumes stable system performance (Chakravarthi et al., 2024[4]). It is crucial to confirm these interpolated results with further experimental data or complex numerical simulations. These presumptions highlight the need for careful interpretation of interpolated data, especially when it comes to crucial design and financial decisions involving wave-powered desalination plants. Particularly when it comes to specific energy consumption (SEC) and water production, the outcomes for the OSWEC and RM3 devices are mostly consistent with those documented in the literature for conventional wave-powered desalination systems. While the RM3's ideal SEC (2–3 kWh/m³) is comparable to other point absorber devices as Delbuoy and CETO (Hicks et al., 1989 [18]; Leijon and Bostrom, 2017[22]), the OSWEC's SEC values (2–4.5 kWh/m³) and water quality are comparable to surge-type WECs that have been previously examined (Chakravarthi et al., 2024). These findings confirm the simulation model's potential to accurately represent WEC performance.

3.2.3. Recommendations and Future Work

The results of this study allow for the formulation of a number of suggestions and possibilities for further research. Firstly, future design improvements should concentrate on increasing the OSWEC device's efficiency in low to moderate wave situations, as it seems more appropriate for reliable desalination performance in the majority of coastal areas. Efforts should be made to increase the RM3 device's operating window, possibly by improving geometry or PTO control techniques to harness more energy in calm waters. To better represent actual deployment settings, both models would benefit from including more thorough PTO subsystems, such as potential electrical conversion or hybrid storage. More thorough modeling of the reverse osmosis unit is also advised, taking into account factors like changing salt concentrations, temperature impacts, and long-term membrane fouling. Physical experiments or field data should be used to further validate the models, especially to verify the accuracy of the dynamic coupling between the desalination unit and WEC. The sea state matrix might be expanded, more extreme or changeable circumstances could be included, and the effects of storm occurrences or device survival could be examined in further simulations. Lastly, future research should incorporate economic and environmental evaluations, taking into account not only technical performance but also the sustainability and cost-effectiveness of large-scale wave-powered desalination implementation.

Future studies should improve the interpolation approach by using more experimental data or numerical simulations to validate interpolated results. Using advanced methods to properly depict complicated nonlinear system behaviors, like polynomial fitting, could increase the accuracy of interpolation. It is also advised to carefully examine interpolation limitations and accuracy using sensitivity analysis, especially in cases of extrapolation and close to borders. Reliability would be further increased by integrating irregular or extreme wave circumstances and expanding the interpolation to a larger variety of sea states. Finally, more precise instructions regarding the precision and relevance of anticipated outcomes would be provided by integrating statistical uncertainty or error estimate techniques into future interpolation projects.

In the future, more simulations and practical testing covering a larger variety of sea conditions should be carried out in order to validate the interpolation process. Predictions for intermediate sea states may become more accurate and reliable if sophisticated interpolation techniques like polynomial surface fitting are incorporated (Leijon and Bostrom, 2017[22]). To assess uncertainties and gain a better understanding of the dependability of the estimated SEC and water production figures, it is advised to include sensitivity analyses and error estimations. Future forecasts would be strengthened if operational factors such as device durability, membrane fouling, and long-term efficiency changes under practical circumstances were addressed (Chakravarthi et al., 2024[4]). In order to enable well-informed decisions for sustainable implementation in coastal communities, it is necessary to conduct economic and environmental assessments of these interpolated data in order to determine the feasibility of commercializing wave-powered desalination. Future studies should recalculate hydrodynamic parameters for each unique site in order to examine the effects of varying water depths. More precise, site-specific evaluations of WEC device performance would be possible with the inclusion of water depth change. This strategy would maximize device selection for various coastal locations and increase the results applicability for real-world deployments.

4

Conclusion

This thesis evaluated two wave energy converters for reverse osmosis-based saltwater desalination: the OSWEC oscillating surge device and the RM3 heaving point absorber. Using matrices, the primary objective was to assess their permeate concentration, water production and Specific Energy Consumption (SEC) performance under varying sea conditions.

The performance of the RM3 device was highly variable. Low efficiency in calmer waters was indicated by its high SEC values at lower wave heights (1–2 meters) and shorter wave periods (5–6 seconds). The RM3's SEC greatly improved with increasing wave heights and periods, reaching ideal values of 2–3 kWh/m³ at higher energy sea states. Similarly, the RM3 produced very little water at low sea states but a lot at extreme wave situations, surpassing 3000 m³/day. According to these findings, the RM3 device works very effectively, but only in limited strong wave conditions.

On the other hand, the OSWEC device showed steady and reliable operation in a wider variety of sea conditions. Even at moderate wave times and lower wave heights, its SEC stayed around 2 to 4.5 kWh/m³. Furthermore, in all studied sea condition, OSWEC continuously generated significant amounts of freshwater, ranging from roughly 300 m³/day in low-energy sea states to over 3500 m³/day in energetic conditions. This stability demonstrates how adaptable and suitable the OSWEC is for locations that have diverse wave conditions. These results are in good alignment with previous studies on related devices. While the RM3's reliance on high-energy conditions is consistent with usual outcomes from point absorber technologies, the OSWEC's steady performance is in line with previous oscillating surge systems (Chakravarthi et al., 2024[4]; Leijon and Boström, 2018[22]). In the majority of sea states, the OSWEC device meets drinking water requirements by achieving permeate concentrations far below 600 ppm. The RM3 device, on the other hand, only reaches these values in the energetic wave conditions.

There are a number of assumptions and restrictions to take into account. The interpolation approach might overlook nonlinear impacts in real ocean conditions since it assumes linear changes between simulated sea states. Hydrodynamic coefficients from idealized frequency-domain BEM solvers are used in the numerical simulations, which may simplify interactions in the real world.

More accurate interpolation techniques, may increase the accuracy of predictions between tested sea states in future investigations. The reliability and application of results might be improved by extending simulations to encompass a wider range of sea conditions, experimental validation and adding realistic operational considerations such membrane fouling or fluctuating salt concentrations.

In conclusion, the study offers strong evidence of the viability of wave-powered desalination. The OSWEC is very promising for real-world application because of its strong and reliable performance in a variety of sea conditions. Although the RM3 device works well in active environments, some environmental factors must be taken into account. These discoveries have the potential to influence future advancements, assisting in the optimization of wave-powered desalination systems to sustainably provide freshwater demands worldwide.

References

[1] George Biddell Airy. “Tides and Waves”. In: *Encyclopedia Metropolitana*. Vol. 5. London, 1845, pp. 241–396.

[2] Aurélien Babarit. “A database of capture width ratio of wave energy converters”. In: *Renewable Energy* 80 (2015), pp. 610–628. DOI: 10.1016/j.renene.2015.02.049. URL: https://www.sciencedirect.com/science/article/pii/S0960148115001652.

[3] C. Beels et al. “Wave energy resource in the North Sea”. In: *Proceedings of the 7th European Wave and Tidal Energy Conference (EWTEC)*. Porto, Portugal, 2007, pp. 507–513. URL: https://repositorio.lneg.pt/bitstreams/0850c309-fc54-4174-84c5-1006bdef1964/download.

[4] T. V. S. Kalyan Chakravarthi, Abhijit Chaudhuri, and Abdus Samad. “Wave Powered Desalination Systems - Recent Developments”. In: *2024 International Conference on Sustainable Energy: Energy Transition and Net-Zero Climate Future (ICUE 2024)*. Available via TU Delft Library. Pattaya City, Thailand: IEEE, 2024, pp. 1–10.

[5] Catherine Charcosset. “A review of membrane processes and renewable energies for desalination”. In: *Desalination* 245 (2009), pp. 214–231. DOI: 10.1016/j.desal.2008.06.020. URL: https://doi.org/10.1016/j.desal.2008.06.020.

[6] Denver Cheddie et al. “Transient modeling of wave powered reverse osmosis”. In: *Desalination* 260 (2010), pp. 153–160. DOI: 10.1016/j.desal.2010.04.048. URL: https://www.sciencedirect.com/science/article/pii/S0011916410002911.

[7] A. Corsini, E. Tortora, and E. Cima. “Preliminary assessment of wave energy use in an off-grid Minor Island desalination plant”. In: *Energy Procedia* 82 (2015), pp. 789–796. DOI: 10.1016/j.egypro.2015.11.813. URL: https://doi.org/10.1016/j.egypro.2015.11.813.

[8] Joao Cruz. *Ocean Wave Energy: Current Status and Future Perspectives*. Berlin, Heidelberg: Springer, 2008. URL: https://books.google.com/books?id=XVBNCexCjoUC.

[9] W. E. Cummins. “The Impulse Response Function and Ship Motions”. In: *Schiffstechnik* 9.47 (1962), pp. 101–109. URL: https://cir.nii.ac.jp/crid/1571417125463837696.

[10] S.A.R.O.S. Desalination. *SAROS–Turning Waves into Fresh Water*. https://sarosdesalination.com/. Accessed: 09 February 2025. 2016.

[11] Menachem Elimelech and William A. Phillip. “The future of seawater desalination: Energy, technology, and the environment”. In: *Science* 333.6043 (2011), pp. 712–717. DOI: 10.1126/science.1200488.

[12] M. Folley and T. Whittaker. “The cost of water from an autonomous wave-powered desalination plant”. In: *Renewable Energy* 34 (2009), pp. 75–81. DOI: 10.1016/j.renene.2008.03.009. URL: https://doi.org/10.1016/j.renene.2008.03.009.

[13] Matt Folley, Baltasar Peñate Suarez, and Trevor Whittaker. “An autonomous wave-powered desalination system”. In: *Desalination* 220.1 (2008). European Desalination Society and Center for Research and Technology Hellas (CERTH), Sani Resort 22 –25 April 2007, Halkidiki, Greece, pp. 412–421. ISSN: 0011-9164. DOI: https://doi.org/10.1016/j.desal.2007.01.044. URL: https://www.sciencedirect.com/science/article/pii/S0011916407006406.

[14] Noreddine Ghaffour, Thomas M. Missimer, and Gary L. Amy. “Technical review and evaluation of the economics of water desalination: Current and future challenges for better water supply sustainability”. In: *Desalination* 309 (2013), pp. 197–207. DOI: 10.1016/j.desal.2012.10.015. URL: https://www.sciencedirect.com/science/article/pii/S0011916412005723.

[15] Giuseppe Giorgi and John V. Ringwood. “Comparing nonlinear hydrodynamic forces in heaving point absorbers and oscillating wave surge converters”. In: *Journal of Ocean Engineering and Marine Energy* 4 (2018), pp. 25–35. DOI: 10.1007/s40722-017-0098-2. URL: https://link.springer.com/article/10.1007/s40722-017-0098-2.

[16] Matthew Hall and collaborators. *MoorDyn [Computer software]*. https://github.com/mattEhall/MoorDynF. Version 2.0, Accessed April 2025. 2024.

[17] K. Hasselmann et al. *Measurements of Wind-Wave Growth and Swell Decay during the Joint North Sea Wave Project (JONSWAP)*. Tech. rep. 12. Hamburg, Germany: Deutsche Hydrographische Zeitschrift, Ergänzungsheft Reihe A(8), 1973. URL: https://pure.mpg.de/pubman/faces/ViewItemOverviewPage.jsp?itemId=item_3262854.

[18] Douglas C. Hicks et al. "DELBUOY: Ocean Wave-Powered Seawater Reverse Osmosis Desalination System". In: *Desalination* 73 (1989), pp. 81–94. DOI: 10.1016/0011-9164(89)87006-7. URL: https://www.sciencedirect.com/science/article/pii/0011916489870067.

[19] Scott Jenne et al. *HERO WEC V1: Design and Experimental Data Collection Efforts*. Tech. rep. NREL/TP-5700-91741. Golden, CO: National Renewable Energy Laboratory, Dec. 2024. DOI: https://www.nrel.gov/docs/fy25osti/91741.pdf.

[20] J. M. J. Journée and W. W. Massie. *Offshore Hydromechanics*. Delft: Delft University of Technology, 2001, p. 523.

[21] N. Lavars. *The Odyssée desalinator: using the power of the ocean to cleanse its own salty waters*. http://newatlas.com/odysse-desalinator-power-ocean-clean/35276/. Accessed: 11 February 2025. 2014.

[22] Mats Leijon and Cecilia Boström. "Freshwater production from the motion of ocean waves–A review". In: *Desalination* 435 (2018), pp. 161–171. DOI: 10.1016/j.desal.2017.12.035. URL: https://www.sciencedirect.com/science/article/pii/S0011916417314455.

[23] Carnegie Wave Energy Limited. *Perth Project*. http://carnegiewave.com/projects/perth-project-2/. Accessed: 09 February 2025. 2015.

[24] Hesham R Lotfy, Jan Staš, and Hynek Roubík. "Renewable energy powered membrane desalination—review of recent development". In: *Environmental Science and Pollution Research* 29.31 (2022), pp. 46552–46568.

[25] Lilian Malaeb and George M. Ayoub. "Reverse osmosis technology for water treatment: State of the art review". In: *Desalination* 267 (2011), pp. 1–8. DOI: 10.1016/j.desal.2010.09.001. URL: https://www.sciencedirect.com/science/article/pii/S0011916410006351.

[26] José Morillo et al. "Comparative study of brine management technologies for desalination plants". In: *Desalination* 336 (2014), pp. 32–49. DOI: 10.1016/j.desal.2013.12.038. URL: https://www.sciencedirect.com/science/article/pii/S0011916414000071.

[27] World Health Organization. *Guidelines for Drinking-water Quality, 4th edition, incorporating the 1st addendum*. Geneva: World Health Organization, 2017. URL: https://www.who.int/publications/i/item/9789241549950.

[28] Justin Panzarella, Toan Tran, and Scott Jenne. *HERO WEC V1. 0 2024-WEC-Sim Detailed Simulation Runs and Summary Data*. Tech. rep. Marine and Hydrokinetic Data Repository (MHKDR); National Renewable Energy …, 2024.

[29] Projet Odysée. *Le Projet Odyssée*. http://projetodyssee.com/. Accessed: 11 February 2025. 2014.

[30] Liliana Rusu, Florin Onea, and Eugen Rusu. "The expected impact of marine energy farms operating in island environments with mild wave energy resources—a case study in the Mediterranean Sea". In: *Inventions* 6.2 (2021), p. 33.

[31] N. Sharmila et al. "Wave powered desalination system". In: *Energy* 29 (2004), pp. 1659–1672. DOI: 10.1016/j.energy.2004.03.099. URL: https://doi.org/10.1016/j.energy.2004.03.099.

[32] R. Suchithra et al. "Numerical modelling and design of a small-scale wave-powered desalination system". In: *Ocean Engineering* 256 (2022), p. 111419. DOI: 10.1016/j.oceaneng.2022.111419. URL: https://www.sciencedirect.com/science/article/pii/S0029801822008010.

[33] WEC-Sim Development Team. *BEMIO [Computer software]*. https://github.com/WEC-Sim/bemio. Accessed March 2025. 2024.

[34] WEC-Sim Development Team. *WEC-Sim (Wave Energy Converter Simulator) [Computer software]*. https://github.com/WEC-Sim/WEC-Sim. Version 5.2.0, Accessed January 2025. 2024.

[35] WEC-Sim Development Team. *WEC-Sim Applications [Computer software]*. https://github.com/WEC-Sim/WEC-Sim_Applications. Accessed March 2025. 2024.

[36] The MathWorks, Inc. *MATLAB R2024a*. The MathWorks, Inc. Natick, Massachusetts, United States, 2024. URL: https://www.mathworks.com/products/matlab.html.

[37] Inc. WAMIT. *WAMIT: A Radiation-Diffraction Panel Program for Wave-Body Interactions [Computer software]*. Version 7.3, Available at https://www.wamit.com/manual.htm, Accessed February 2025. Chestnut Hill, MA, 2016.

[38] UN Water. *Water Scarcity*. Retrieved from https://www.unwater.org/water-facts/scarcity. 2023.

[39] M. Ylänen and M.J. Lampinen. "Determining optimal operating pressure for AaltoRO a novel wave powered desalination system". In: *Renewable Energy* 69 (2014), pp. 386–392. DOI: 10.1016/j.renene.2014.03.061. URL: https://doi.org/10.1016/j.renene.2014.03.061.

[40] Diab Yousri M et al. "A Comprehensive Review of Promising Hybrid Sea Waves Energy Powered Desalination Techniques". In: *World of Science: Journal on Modern Research Methodologies* 2.7 (2023), pp. 59–70.

[41] Yi-Hsiang Yu and Dale Jenne. "Analysis of a Wave-Powered, Reverse-Osmosis System and Its Economic Availability in the United States: Preprint". In: *Proceedings of the 36th International Conference on Ocean, Offshore and Arctic Engineering (OMAE 2017)*. NREL/CP-5000-67973. Available at https://www.nrel.gov/docs/fy17osti/67973.pdf. National Renewable Energy Laboratory (NREL). Trondheim, Norway: American Society of Mechanical Engineers (ASME), 2017, OMAE2017–62136.

[42] Yi-Hsiang Yu and Dale Jenne. "Numerical Modeling and Dynamic Analysis of a Wave-Powered Reverse-Osmosis System". In: *Journal of Marine Science and Engineering* 6.132 (2018), pp. 1–17. DOI: 10.3390/jmse6040132. URL: https://www.mdpi.com/2077-1312/6/4/132.

[43] Iñaki Zabala et al. "BEMRosetta: An open-source hydrodynamic coefficients converter and viewer integrated with Nemoh and FOAMM". In: *Proceedings of the 14th European Wave and Tidal Energy Conference (EWTEC 2021)*. Plymouth, UK, 2021.

[44] Mohd Muzammil Zubair, Haleema Saleem, and Syed Javaid Zaidi. "Recent progress in reverse osmosis modeling: An overview". In: *Desalination* 564 (2023), p. 116705. DOI: 10.1016/j.desal.2023.116705. URL: https://www.sciencedirect.com/science/article/pii/S0011916423003375.

A

WECSim Input code

```
1
2 %% Simulation Data
3 simu = simulationClass();
4 simu.simMechanicsFile = 'RM3.slx';      % Specify Simulink Model File
5 %simu.mode = 'rapid-accelerator';           % Specify Simulation Mode
      ('normal','accelerator','rapid-accelerator')
6 simu.explorer='on';                          % Turn SimMechanics Explorer (on/off)
7 simu.solver = 'ode4';                         %simu.solver = 'ode4' for fixed step
      & simu.solver = 'ode45' for variable step
8 simu.startTime = 0;                           % Simulation Start Time [s]
9 simu.rampTime = 250;
10 simu.endTime= 1000;
11 simu.dt = 0.01;                              %Simulation time-step [s] for a
      convolution function in the radiation force calculation
12 simu.cicEndTime = 30;
13
14 % Irregular Waves using JS Spectrum with Equal Energy and Seeded Phase
15 waves = waveClass('irregular');           % Initialize Wave Class and Specify Type
16 waves.height = [1, 2, 3, 4, 5];    %[1.0, 2.0, 3.0, 4.0, 5.0];
                              % Wave Height [m]
17 waves.period = 1.1*[5, 6, 7, 8, 9];       %1.1*[4.65, 5.81, 6.97, 8.13, 9.30];
                                % Wave Period [s]
18 waves.spectrumType = 'JS';                % Specify Wave Spectrum Type
19 waves.bem.option = 'EqualEnergy';         % Uses 'EqualEnergy' bins (default)
20 waves.phaseSeed = 1;                      % Phase is seeded so eta is the same
21 waves.gamma = 3.3;                        % Explicitly set peak enhancement factor
22
23 %% Body Data
24 % Float
25 body(1) = bodyClass('hydroData/rm3.h5');
26     % Create the body(1) Variable, Set Location of Hydrodynamic Data File
27     % and Body Number Within this File.
28 body(1).geometryFile = 'geometry/float.stl';    % Location of Geomtry File
29 body(1).mass = 'equilibrium';
30     % Body Mass. The 'equilibrium' Option Sets it to the Displaced Water
31     % Weight.
32 body(1).inertia = [20907301 21306090.66 37085481.11];  % Moment of Inertia
      [kg*m^2]
33
34 % Spar/Plate
35 body(2) = bodyClass('hydroData/rm3.h5');
36 body(2).geometryFile = 'geometry/plate.stl';
37 body(2).mass = 'equilibrium';
```

```
body(2).inertia = [94419614.57 94407091.24 28542224.82];

%% PTO and Constraint Parameters
% Floating (3DOF) Joint
constraint(1) = constraintClass('Constraint1'); % Initialize Constraint Class for
    Constraint1
constraint(1).location = [0 0 0];               % Constraint Location [m]

% Translational PTO
pto(1) = ptoClass('PTO1');                      % Initialize PTO Class for PTO1
pto(1).stiffness = 0;                           % PTO Stiffness [N/m]
pto(1).damping = 1200000*0;                       % PTO Damping [N/(m/s)]
pto(1).location = [0 0 0];                      % PTO Location [m]

%% Mooring
% Moordyn
mooring(1) = mooringClass('mooring');           % Initialize mooringClass
mooring(1).moorDyn = 1;                         % Initialize MoorDyn
mooring(1).moorDynLines = 6;                    % Specify number of lines
mooring(1).moorDynNodes(1:3) = 16;              % Specify number of nodes per line
mooring(1).moorDynNodes(4:6) = 6;               % Specify number of nodes per line
mooring(1).initial.displacement = [0 0 -21.29-.21]; % Initial Displacement (body
    cg + body initial displacement)
```

Listing A.1: WECSim Input code for Heaving WEC device

```

%% Simulation Data
simu = simulationClass();
simu.simMechanicsFile = 'OSWEC.slx';      % Specify Simulink Model File
%simu.mode = 'rapid-accelerator';           % Specify Simulation Mode
    ('normal','accelerator','rapid-accelerator')
simu.explorer='on';                         % Turn SimMechanics Explorer (on/off)
simu.solver = 'ode4';                       %simu.solver = 'ode4' for fixed step
    & simu.solver = 'ode45' for variable step
simu.startTime = 0;                         % Simulation Start Time [s]
simu.rampTime = 250;
simu.endTime=1000;
simu.dt = 0.01;                             %Simulation time-step [s] for a
    convolution function in the radiation force calculation
simu.cicEndTime = 30;
% Irregular Waves using JS Spectrum with Equal Energy and Seeded Phase
waves = waveClass('irregular');             % Initialize Wave Class and Specify Type
waves.height = [1, 2, 3, 4, 5];     %[1.0, 2.0, 3.0, 4.0, 5.0];
                          % Wave Height [m]
waves.period = 1.1*[5, 6, 7, 8, 9];       %1.1*[4.65, 5.81, 6.97, 8.13, 9.30];
                            % Wave Period [s]
waves.spectrumType = 'JS';                  % Specify Wave Spectrum Type
waves.bem.option = 'EqualEnergy';           % Uses 'EqualEnergy' bins (default)
waves.phaseSeed = 1;                        % Phase is seeded so eta is the same
waves.gamma = 3.3;                          % Explicitly set peak enhancement factor
%% Body Data
% Flap
body(1) = bodyClass('hydroData/oswec.h5');   % Initialize bodyClass for Flap
body(1).geometryFile = 'geometry/flap.stl';  % Geometry File
body(1).mass = 127000;                         % User-Defined mass [kg]
body(1).inertia = [1.85e6 1.85e6 1.85e6]; % Moment of Inertia [kg-m^2]
body(1).morisonElement.option = 1;
body(1).morisonElement.cd = ones (5,3);
body(1).morisonElement.ca = zeros(5,3);
body(1).morisonElement.area = zeros(5,3);
```

```
body(1).morisonElement.area(:,1) = 18*1.8;
body(1).morisonElement.area(:,3) = 18*1.8;
body(1).morisonElement.VME  = zeros(5,1);
body(1).morisonElement.rgME = [0 0 -3; 0 0 -1.2; 0 0 0.6; 0 0 2.4; 0 0 4.2];
% Base
body(2) = bodyClass('hydroData/oswec.h5');   % Initialize bodyClass for Base
body(2).geometryFile = 'geometry/base.stl';  % Geometry File
body(2).mass = 999;                            % Placeholder mass for fixed body
body(2).inertia = [999 999 999];               % Placeholder inertia for fixed
    body
%% PTO and Constraint Parameters
constraint(1)= constraintClass('Constraint1'); % Initialize ConstraintClass
constraint(1).location = [0 0 -10];
constraint(2)= constraintClass('Constraint2'); % Initialize ConstraintClass
constraint(2).location = [0 0 -8.9];
constraint(3)= constraintClass('Constraint3'); % Initialize ConstraintClass
constraint(3).location = [4.7021271782+0.9 0 -8.7];
constraint(4)= constraintClass('Constraint4'); % Initialize ConstraintClass
constraint(4).location = [0+0.9 0 -7];
pto(1) = ptoClass('PTO1');                     % Initialize ptoClass for PTO1
pto(1).stiffness = 0;                          % PTO Stiffness Coeff [Nm/rad]
pto(1).damping = 1200000*0;                            % PTO Damping Coeff
    [Nsm/rad]
pto(1).location = [2.35106397378+0.9 0 -7.849998936];   % PTO Global Location [m]
pto(1).orientation.z = [-4.7021271782/5 0 1.7/5];       % PTO orientation
```

Listing A.2: WECSim Input code for Oscillating Surge WEC device

B

WECSim User Defined Functions code

```
% Define filename to save per case
filename = sprintf('OSWEC%03d.mat', imcr);

% === Set steady-state time window ===
t_start = 500;  % [s]
t_end = 1000;    % [s]

% Extract time index range for steady-state
idx = (simout.time >= t_start) & (simout.time <= t_end);
dt = mean(diff(simout.time(idx)));

% Extract mechanical signals from simout
velocity    = abs(simout.signals.values(idx,1));   % [m/s]
force       = abs(simout.signals.values(idx,2));   % [N]
mech_power  = abs(simout.signals.values(idx,3));   % [W]

% Extract RO output (permeate flow) from simout1
permeate_flow = simout1.signals.values(idx,2); % [m³/s]

% === Time-averaged values ===
mcr.avgVelocity(imcr)     = mean(velocity);
mcr.avgForce(imcr)        = mean(force);
mcr.avgMechPower(imcr)    = mean(mech_power);      % [W]
mcr.avgWaterProd(imcr)    = mean(permeate_flow);   % [m³/s]

% === Derived Metrics ===
% Convert to more useful units
avg_power_kW = mcr.avgMechPower(imcr) / 1000;               % [kW]
avg_water_m3day = mcr.avgWaterProd(imcr) * 86400;           % [m³/day]

% Specific Water Production [m³/kWh]
mcr.SWP(imcr) = avg_water_m3day / (avg_power_kW * 24);      % over 24 hr

% Specific Energy Consumption [kWh/m³]
mcr.SEC(imcr) = (avg_power_kW * 24) / avg_water_m3day;

%  Constants
Cm = 35946;                     % [mg/L] Seawater concentration
A_m = 35.3;                     % [m^2] Membrane area per module
N_mem = 183;                    % [-] Number of membranes
A_tot = A_m * N_mem;            % [m^2] Total area
A_omega = 1e-11;                % [m/(s·Pa)] Water permeability (typical)
Bs = 3e-8;                      % [m/s] Solute permeability (typical)
```

```
44
45 % Calculate (DeltaP - DeltaPi) using measured permeate flow
46 deltaP_minus_deltaPi = permeate_flow ./ (A_omega * A_tot);
47
48 % Calculate permeate concentration Cp (mg/L or ppm)
49 Cp = Cm ./ ((A_omega / Bs) * deltaP_minus_deltaPi + 1);
50
51 % Save time-averaged value for this MCR case
52 mcr.avgPPM(imcr) = mean(Cp);
53
54 % Save intermediate results
55 save(filename, 'mcr', 'simout', 'simout1');
56
57  % Final plotting
58 if imcr == length(mcr.cases)
59     Hs = mcr.cases(:,1);  % Significant wave height [m]
60     Te = mcr.cases(:,2);  % Energy period [s]
61
62     % Reshaping dimensions
63     unique_Hs = unique(Hs);
64     unique_Te = unique(Te);
65     l_waveheight = length(unique_Hs);
66     l_waveperiod = length(unique_Te);
67
68     % Reshape and plot heatmaps
69     vars = {mcr.avgVelocity, mcr.avgForce, mcr.avgMechPower, mcr.avgWaterProd *
           86400, mcr.SWP, mcr.SEC, mcr.avgPPM};
70     titles = { 'Avg Velocity [m/s]', 'Avg Force [N]', 'Avg Mechanical Power [W]',
           'Avg Water Production [m³/day]', 'Specific Water Production [m³/kWh]',
           'Specific Energy Consumption [kWh/m³]', 'Average Permeate Concentration
           [ppm]'};
71     filenames = { 'Velocity', 'Force', 'Power', 'WaterProd', 'SWP',
           'SEC','Permeate Concentration' };
72
73     for i = 1:length(vars)
74         data_matrix = reshape(vars{i}, [l_waveperiod, l_waveheight])';
75         figure;
76         heatmap(data_matrix, 'XData', unique_Te, 'YData', unique_Hs);
77         xlabel('Te [s]');
78         ylabel('Hs [m]');
79         title(titles{i});
80     end
81 end
```

Listing B.1: User Defined Functions code for both devices

C

Simulink Models

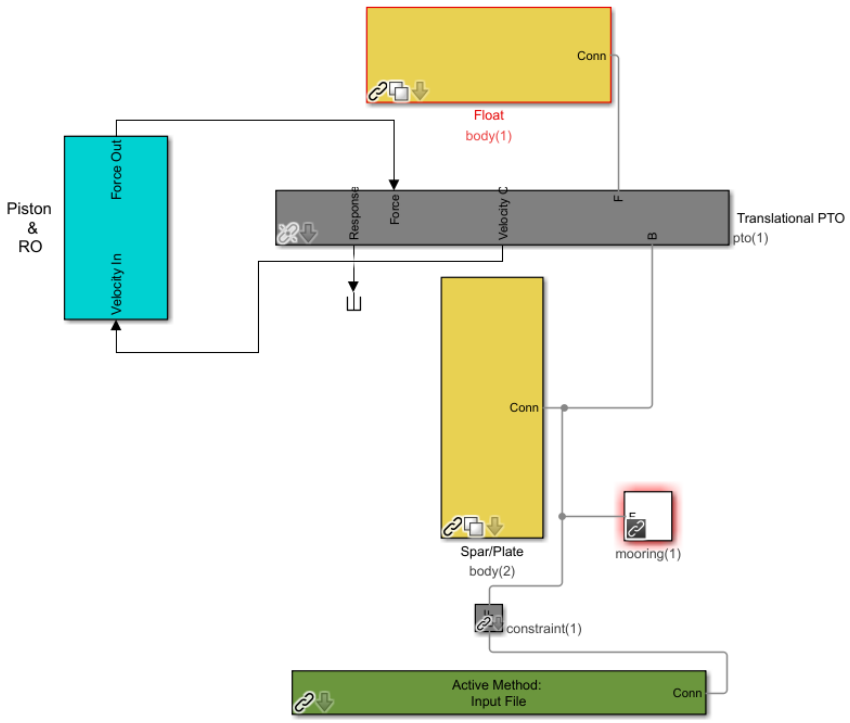

Figure C.1: Modified Simulink model for RM3 Heaving device

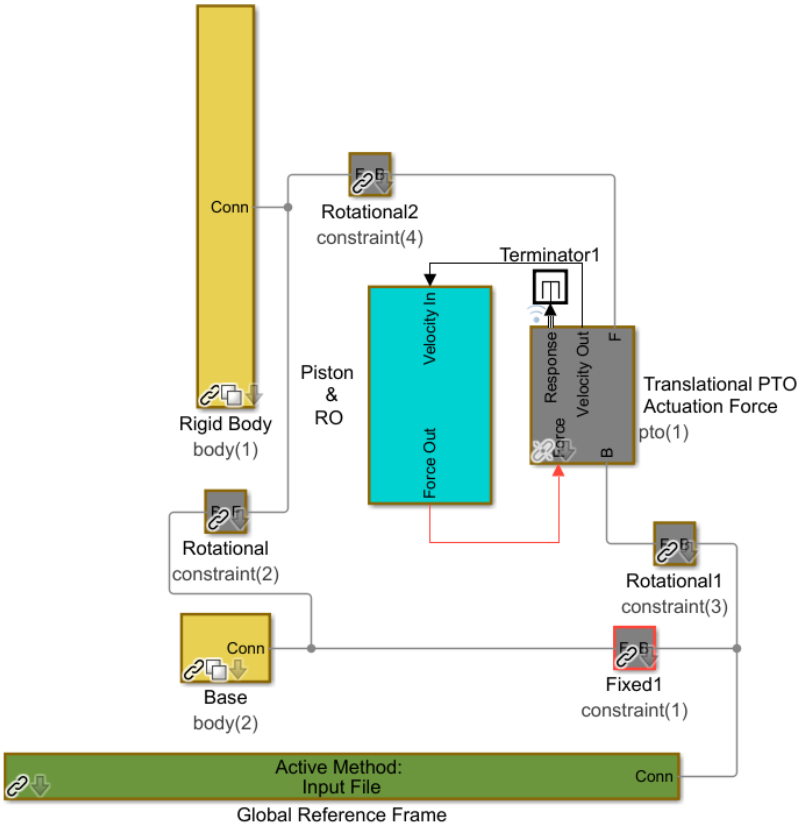

Figure C.2: Modified Simulink model for OSWEC device

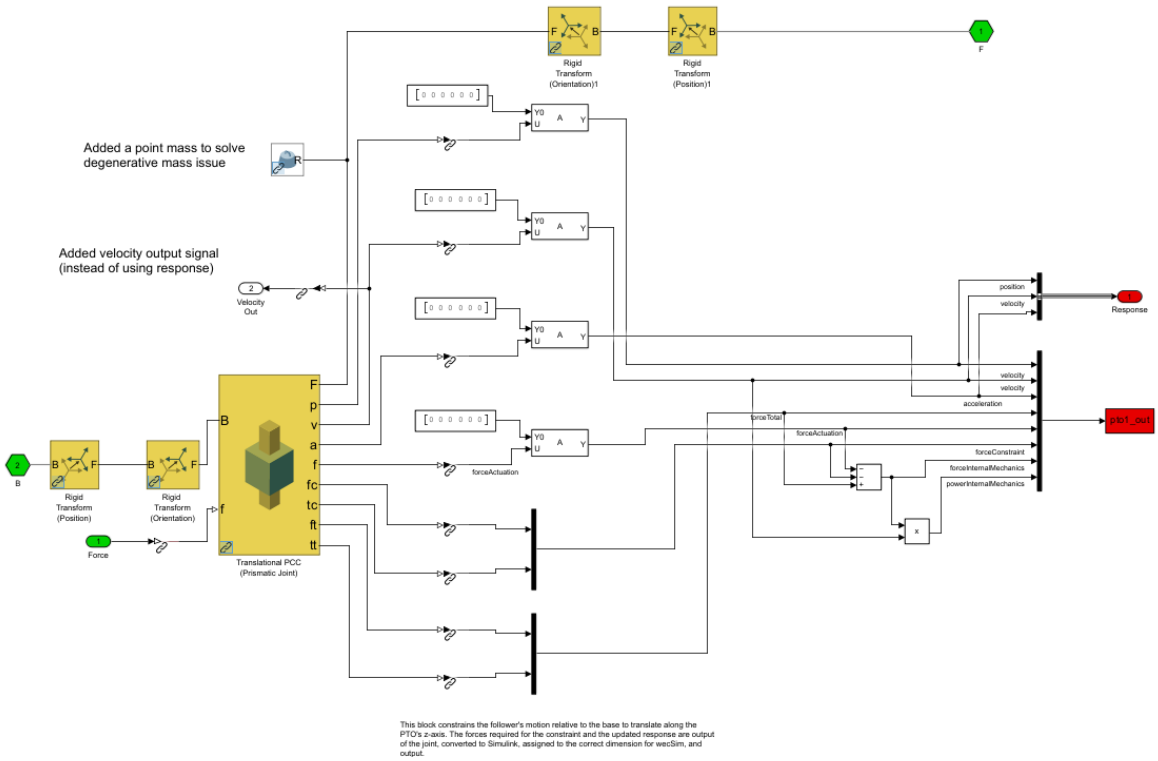

Figure C.3: Translational PTO Simulink Model

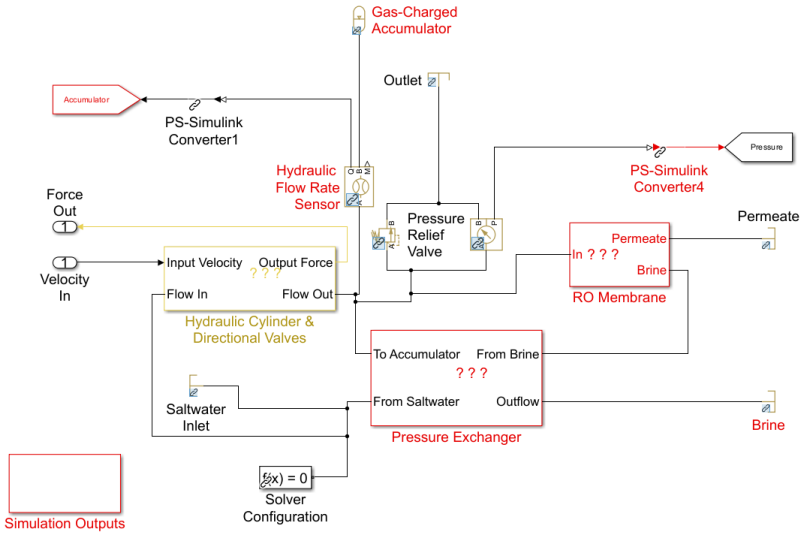

Figure C.4: Piston and RO Simulink Model

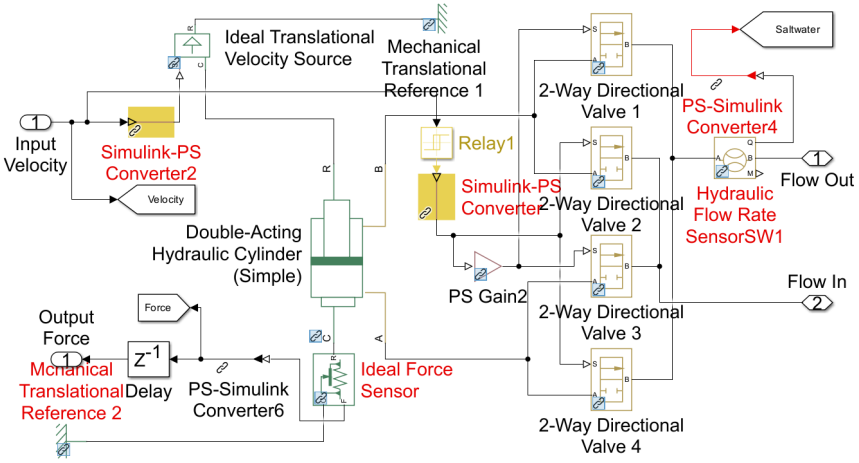

Figure C.5: Hydraulic Cylinder and Directional Valves Simulink Model

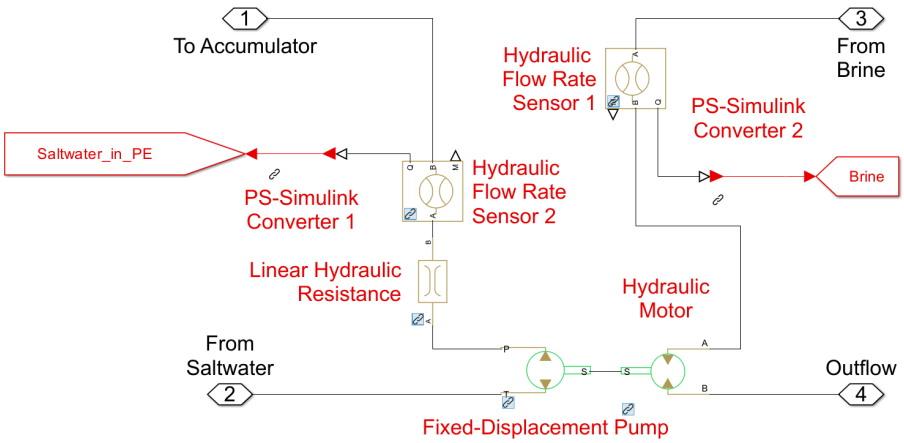

Figure C.6: Pressure Exchanger Simulink Model

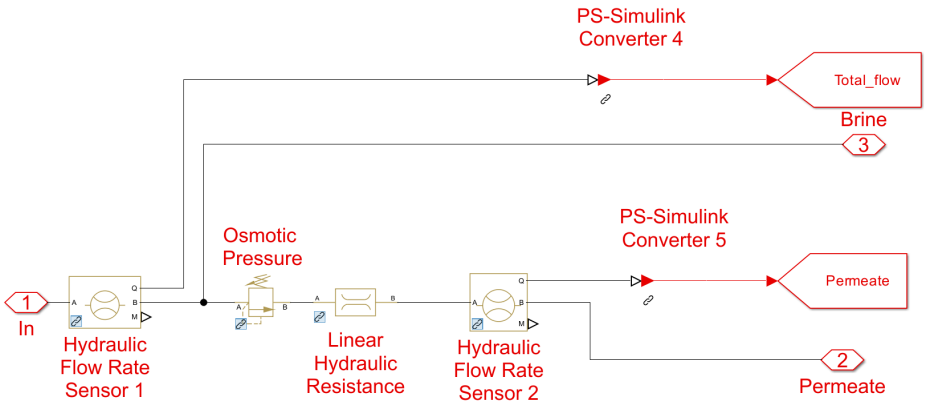

Figure C.7: RO Membrane Simulink Model

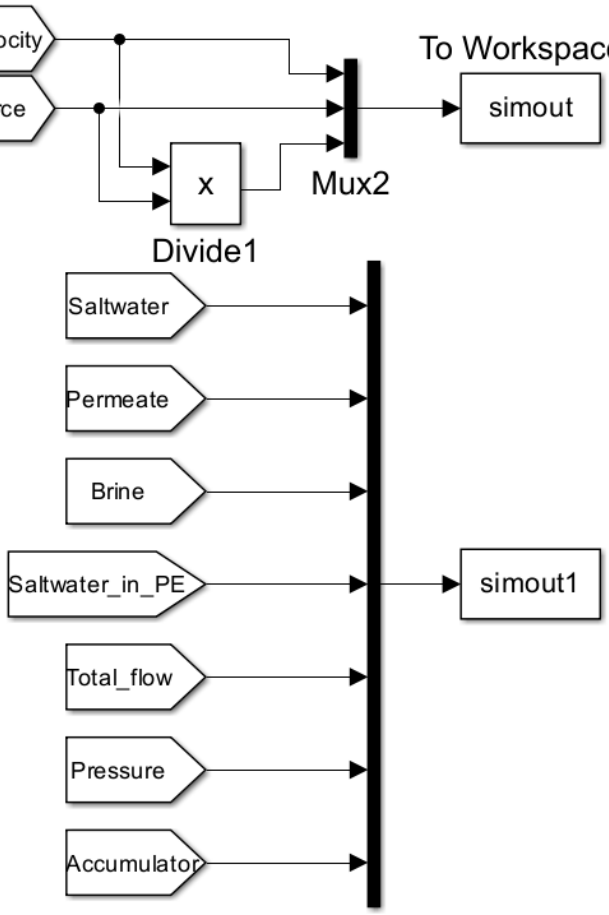

Figure C.8: Simulation Outputs Simulink Model

D

Interpolation Framework

```
1
2  % Values from the simulations
3  Hs_values = [1 2 3 4 5]; % Significant wave height [m]
4  Te_values = [5 6 7 8 9]; % Energy period [s]
5
6  % SEC matrix [kWh/m^3] from the power matrix results
7  SEC_matrix = [
8      1.754e7, 2.606e7, 171.1,   23.67,  3.333;
9      52.17,   3.171,   2.013,   2.109,  1.818;
10     2.776,   1.98,    2.128,   2.323,  2.416;
11     2.191,   2.125,   2.738,   3.012,  3.11;
12     2.103,   2.778,   3.779,   4.077,  4.031
13 ];
14
15 % Average Water Production matrix [m^3/day]
16 WaterProd_matrix = [
17     3.278e-6, 3.802e-6, 1.046,   11.79,  150.7;
18     4.62,     161.6,    663.1,   979,    1315;
19     286.1,    1034,     1823,    2102,   2330;
20     952,      2025,     2669,    2920,   2811;
21     1706,     2686,     3133,    3191,   3059
22 ];
23
24 % Desired interpolation values
25 Hs_query = 3.5; % wave height
26 Te_query = 7.5; % energy period
27
28 % Bilinear interpolation
29 SEC_interpolated = interp2(Te_values, Hs_values, SEC_matrix, Te_query, Hs_query,
       'linear');
30 WaterProd_interpolated = interp2(Te_values, Hs_values, WaterProd_matrix,
       Te_query, Hs_query, 'linear');
31
32 % Display the interpolated results
33 fprintf('Interpolated SEC at Hs=%.2fm, Te=%.2fs: %.3f kWh/m^3\n', Hs_query,
       Te_query, SEC_interpolated);
34 fprintf('Interpolated Water Production at Hs=%.2fm, Te=%.2fs: %.2f m^3/day\n',
       Hs_query, Te_query, WaterProd_interpolated);
```

Listing D.1: Framework used for Interpolation of Matrices